Potential of geoelectrical methods to monitor root zone processes and structure: a review

Mihai Octavian Cimpoiașu[a,b], Oliver Kuras[b], Tony Pridmore[c], Sacha J. Mooney[a]

[a] Division of Agriculture and Environmental Sciences, School of Bioscience, University of Nottingham, Sutton Bonington, Leicestershire, LE12 5RD, UK; [b] Geophysical Tomography Team, British Geological Survey, Keyworth, Nottinghamshire, NG12 5GG, UK; [c] School of Computer Science, University of Nottingham, Wollaton Road, Nottingham, Nottinghamshire, NG8 1BB, UK

Corresponding author: Mihai O. Cimpoiașu

E-mail: mcim@bgs.ac.uk

Address: Nicker Hill, Keyworth, Nottinghamshire, UK

Postcode: NG12 5GG

1 Abstract

2 Understanding the processes that control mass and energy exchanges between soil, plants and the atmosphere plays
3 a critical role for understanding the root zone system, but it is also beneficial for practical applications such as
4 sustainable agriculture and geotechnics. Improved process understanding demands fast, minimally invasive and
5 cost-effective methods of monitoring the shallow subsurface. Geoelectrical monitoring methods fulfil these crite-
6 ria and have therefore become of increasing interest to soil scientists. Such methods are particularly sensitive to
7 variations in soil moisture and the presence of root material, both of which are essential drivers for processes and
8 mechanisms in soil and root zone systems. This review analyses the recent use of geoelectrical methods in the
9 soil sciences, and highlights their main achievements in focal areas such as estimating hydraulic properties and
10 delineating root architecture. We discuss the specific advantages and limitations of geoelectrical monitoring in this
11 context. Standing out amongst the latter are the non-uniqueness of inverse model solution and the appropriate
12 choice of pedotransfer functions between electrical parameters and soil properties. The relationship between geo-
13 electrical monitoring and alternative characterization methodologies is also examined. Finally, we advocate for
14 future interdisciplinary research combining models of root hydrology and geoelectrical measurements. This includes
15 the development of more appropriate analogue root electrical models, careful separation between different root zone
16 contributors to the electrical response and integrating spatial and temporal geophysical measurements into plant
17 hydrological models to improve the prediction of root zone development and hydraulic parameters.

18

19 **Keywords:** *electrical-properties; root zone soil moisture; root system monitoring; root zone structure, root*
20 *detection; modelling; geophysics; geoelectrical methods;*

21 **Conflict of interest**: none

22

23 **Abbreviations**: Electrical Resistivity Tomography (ERT), Electrical Capacitance Method (ECM), Electrical
24 Impedance Spectroscopy (EIS), Electrical Impedance Tomography (EIT), Electo-Magnetic Imaging (EMI), Spectral
25 Induced Polarization (SIP), Induced Polarization (IP), Time-Domain Induced Polarization (TDIP), Frequency-
26 domain Induced polarization (FDIP), Computed Tomography(CT), Ground Penetrating Radar (GPR), Electrical
27 capacitance(EC), Waxman- Smits model (WS), Time Domain Reflectometry (TDR), Water Content (WC), Soil
28 water content (SWC), Root water uptake (RWU).

1   Introduction

Root zone is a term used to describe the region of soil that is directly influenced by plant roots and all its inherent physicochemical processes. It links directly to human activity; for example, agriculture is typically based on anthropic interactions with the root zone. In addition to its economic importance, studying the root zone provides the tools to protect and to nurture a sustainable environment. In order to understand soil-plant interactions, a detailed appreciation is essential of processes such as: root water uptake, growth of micro-organism communities, nutrient fixation, carbon sequestration and soil structure. This requires the development and routine use of well-defined investigation and quantification methods in order to translate the measurable observations into meaningful soil and root parameters, including hydraulic conductivity, porosity, root length, root biomass or soil respiration. Assessment of root zone processes can take place in-situ or ex-situ, with both experimental settings serving different purposes. Laboratory studies allow the creation of a controlled environment with defined media where experimental parameters are carefully planned and adjusted. This can help understand soil processes on a specific, localized scale (typically sub-metre). By contrast, field surveys facilitate the study of processes in an undisturbed setting. In addition, they provide the necessary benchmarks for translating laboratory results into the real environment. They allow evaluation of methods for monitoring natural and man-made inputs to the root zone system, including agricultural strategies such as inter-cropping or crop rotation, which can only be tested at the field scale (100s of metres) (Garré et al., 2012).

Over recent decades, a range of assessment methods for the root zone has been developed. These can be split into invasive/destructive and minimally/non-invasive approaches. Invasive methods disturb the integrity of the soil in order to determine soil (moisture content, calcium content, pH) and root (elongation, mass) properties. Examples include the core-break method (Moreno et al., 2005; Escamilla et al., 1991; Bland, 1989) and the use of minirhizotron tubes (Hendrick and Pretigzer, 1996; Garré et al., 2011). Whilst the results obtained in this way are accurate, useful and do not require ground-truthing, they reflect conditions at the test locality only. Achieving meaningful experimental coverage therefore requires many sampling points, which can be time-consuming and laborious. Furthermore, altering the soil properties through sampling reduces the opportunities for continuously monitoring the soil-plant system.

The literature offers many examples of minimally-invasive methods such as TDR (Michot et al., 2001) and non-invasive methods, including X-ray Computed Tomography (CT) (Peyton et al., 1992), Neutron Probe Imaging (Vrugt et al., 2001) or Magnetic Resonance Imaging (MRI) (Segal et al., 2008). These methods provide important insights concerning soil structure (Peyton et al., 1992) or soil water transport (Amin et al., 1996) and more recently they have allowed imaging of the plant root architecture in situ (Mooney et al., 2012). Even though these technologies provide high resolution 3D results, they are expensive to deploy and maintain. Also, at the current state of technology, they restrict the user to a laboratory environment. The exception is TDR, which is frequently employed in field surveys. However, the spatial coverage and resolution achievable with TDR and other non-invasive methods

63   based on point sensors is comparatively poor.

64   Geoelectrical tomography represent a relatively recent, but fast growing set of tools for soil assessment and monitor-

65   ing. In particular, efficient methods for investigating soil-plant interaction are increasingly in demand. Geoelectrical

66   methods are minimally invasive and involve the use of sensors that penetrate the soil surface only (top 10 cm),

67   thus not disturbing the integrity of the volume under investigation. Well-established methods include: Electrical

68   Resistivity Tomography (ERT), Electrical Impedance Tomography (EIT), Electrical Capacitance Method (ECM)

69   and Induced Polarization (IP) with some conceptual overlap between them. A significant body of research has

70   focused on ERT, due to its robustness and ease of use, particularly in the field. Geoelectrical techniques facilitate

71   both in-situ and ex-situ assessments of soil. The methodology allows comparatively rapid data acquisition which

72   enables near real-time measurements (Loke et al., 2013; Samouëlian et al., 2005). It also allows practically continu-

73   ous measurements over time, which provides an important capability for the long-term monitoring of soil processes.

74   The physical principles governing this family of methods involves electrical current signals driven into the soil

75   through electrodes and subsequent recording of differences in electrical potential associated with the subsurface

76   current flow. Larger arrays of multiple electrodes are typically used to acquire geoelectrical data, with individ-

77   ual measurements made consecutively on small subsets of electrodes. Electrical parameters such as conductivity,

78   polarization or capacitance are measured. The systematic collation of datasets with multiple point measurements

79   allows the application of tomographic imaging techniques, which can generate 2, 3 or even 4 dimensional images

80   of the subsurface distribution of electrical properties. This enables quantification of spatial and temporal property

81   variations within soils.

82   Whilst many factors can influence soil electrical properties (e.g. porosity, density, clay content), a particularly

83   useful application is their use as a proxy for soil water content (SWC; Michot et al. (2001)). SWC quantification is

84   critically important for most soil studies. Firstly, it is indicative of plant water availability (Denmead, 1961) and

85   secondly, it is a major factor controlling soil respiration (Davidson et al., 1998) or soil aggregates stability (Haynes

86   and Beare, 1997). Geoelectrical monitoring is able to quantify temporal variations in SWC, and has been used to

87   monitor plant water uptake in the laboratory (Werban et al., 2008) and in the field (Michot et al., 2003), as well as

88   to monitor soil water availability (Brillante, 2016; Srayeddin and Doussan, 2009).

89   A direct correlation has been found between electrical permittivity and root biomass (Dalton, 1995). Therefore, root

90   presence and activity can be quantified directly from electrical measurements. Moreover, organic matter has the

91   ability to polarize electrical current (Schwan, 1957). Researchers have exploited this for assessing the architecture

92   of root systems by measuring not only conductivity (Amato et al., 2009), but also chargeability (Mary et al., 2017).

93   In this study we review the main opportunities for geoelectrical monitoring in root zone research and discuss the

94   key questions that may be addressed in this way. We also seek to highlight the information each method delivers

95   to the user and appraise the state of the art in terms of geoelectrical instrumentation and methodology for root

96   zone research. Current gaps in knowledge and research needs are identified, covering issues such as the variability

97   of pedotransfer functions, the use of a-priori information to constrain the geoelectrical result and the advantages of

complementing geoelectrical information with GPR or EMI data in a joint field surveying strategy. We conclude with an outlook to future research opportunities within the experimental observation and conceptual modelling of the root zone. Therefore, with a view to advancing our understanding of root zone processes, we suggest the root system requires a more comprehensive electrical analogue representation, the contributors to the geoelectrical response need to be appropriately separated and a coupled research framework aimed to improve root zone parametrization which jointly includes geoelectrical measurements and simulations of plant growth and hydraulic properties.

2 Geoelectrical monitoring - General principles

2.1 Electrical properties of soils and their variability

The application of geoelectrical methods in root zone research aims at determining the electrical properties of soils, namely, conduction and polarization. Electrical conduction represents the movement of electrically charged particles through liquid and solid phases of the soil medium. Their flow will depend on the amount of available charge, the distribution of conducting paths and the charge mobility. Electrical polarization represents the redistribution of positive and negative charges when exposed to an exterior electric field. In consequence, this will determine regions of charge accumulations across the soil medium.

Variability in soil electrical properties can be caused by either inorganic or organic constituents of the soil system. Soil electrical conduction is generally determined by pore fluid and mineral surface conductivity. Soil electrical polarization is determined by the pore architecture and water-mineral interface capacity of ion aggregation (Everett, 2013). Therefore, a number of properties intrinsic to the soil (i.e. its inorganic constituents) have a direct effect on the electrical response. Further essential contributors to the electrical response are components of the root zone with an organic origin, such as decomposed plant material, collectively known as humus, and plant root systems.

2.1.1 Inorganic constituents

Pore fluid. Electrical conduction in soils is mostly electrolytic, ions in the pore fluid being the charge carriers (Everett, 2013). The amount of charges increases with fluid ionic concentration or the volumetric water content given a constant fluid conductivity.

When an electrolyte comes in contact with a charged surface of a soil particle, an electrical double layer (EDL) forms and ions are adsorbed onto the solid surface (Revil and Glover, 1997), therefore affecting ion mobility which gives rise to electrical polarization (Lyklema et al., 1983).

Solid soil. Generally, the solid matrix acts like a semi-conductor with some exceptions such as the surface of clay minerals. Their inherently negative surface charge constitutes another electrical conduction pathway. Also, soils with a predominantly clay texture tend to exhibit a larger specific surface area than soils consisting primarily of sand (Pennell, 2016). Therefore, clay content implies a larger conductive particle surface which leads to an important

130   contribution to the soil electrical conductivity (Fukue et al., 1999).

131   **Air Filled pore space.** The volume (porosity) and connectivity of the pore network determine a soil's water

132   holding capacity, which in turn affects the bulk soil electrical conduction. Also, the tortuous nature of the pore

133   system generates complex patterns of fluid flow which can determine electrically conductive and non-conductive

134   regions. As for polarization, due to the formation of EDLs, narrow pore channels may cause charge accumulation

135   and localized disequilibria in ionic concentration (Revil, 1999).

136   **Temperature.** An increase in pore fluid temperature causes a decrease in pore fluid viscosity, which in turn

137   increases the ion agitation in the solution. Alternatively, in freezing conditions, molecules of salt are rejected into

138   unfrozen pore water, thus changing the concentration of the pore solution (Banin and Anderson, 1974). Superficial

139   soils are exposed to diurnal and seasonal fluctuations in temperature, therefore neglecting such variability may lead

140   to serious errors in geoelectrical data interpretations (Samouëlian et al., 2005).

141   2.1.2   Organic constituents

142   **Organic matter (OM).** The capacity of the soil to retain ions (or ion exchange capacity) is a measure of soil

143   surface charge (Zelazny et al., 1996). A considerable proportion of soil cation exchange capacity (CEC) is associated

144   with soil organic matter. Interactions between OM and soil minerals result in a decrease in ion mobility, and thus

145   a decrease in polarization (Schwartz and Furman, 2015).

146   **Plant roots.** The living root system has a very complex electrical response that depends on root characteristics,

147   such as: mass, length, structure, type (woody or herbaceous) or tortuosity. Woody root tissue does not contain

148   charge carriers therefore their presence in the soil system will reduce the overall bulk electrical conductivity (Van-

149   derborght et al., 2013). However, electrical current will flow through the root xylem as the fluid contains electrical

150   charges. EDLs form both at the contact between the outer and inner root surface, therefore the magnitude of root

151   polarization relates to their overall surface area (Weigand and Kemna, 2018).

152   2.2   Methods of measuring soil electrical properties

153   A range of geoelectrical methods is available to measure soil properties. In this section we aim to provide a short

154   introduction to the physical and functionality principles governing these methods.

155   2.2.1   Complex electrical impedance

156   In practice an electrical measurement on soil involves a measurement of the complex impedance $\hat{Z}$ of the material,

157   a frequency f dependent function expressed as:

$$\hat{Z} = (Z'(\omega) + iZ"(\omega)), \tag{1}$$

158   where i is the imaginary unit, $\omega = 2\pi f$, Z' and $Z"$ are the real and imaginary parts of the impedance respectively.

159   This can in turn be translated into effective material properties by taking into account the dimensions and spatial

160 geometry of the measurement, represented through the geometric factor K. Therefore we can obtain an expression

161 for the 'apparent' complex conductivity $\hat{\sigma}_a$ and its inverse, complex resistivity $\hat{\rho}_a$, which describe how well a material

162 conducts electrical current flow:

$$\hat{\sigma}_a = (K * \hat{Z})^{-1} = \sigma' + i\sigma" = |\rho_a| * e^{-i\phi}, \tag{2}$$

163 where the real part σ' quantifies conduction and $\sigma"$ quantifies polarization. ϕ is the phase angle that represents the

164 phase shift between the injected current and measured voltage.

2.2.2   ERT

166 For this review we selected 72 articles spanning across 22 years (1996-2018) which feature the application of geo-

167 electrical methods in root zone research (Complete list in Appendix A and B). ERT is one of the most extensively

168 used near surface geophysical methods and is also extremely popular for the study of soil-plant interaction. 65% of

169 the studies reviewed for this paper employed ERT as the primary method of imaging soil-plant interaction. ERT

170 applications inject DC or low-frequency current into the soil and tend to measure the magnitude $|\hat{Z}|$ of the electrical

171 impedance only. Provided that the geometric factor K is known, the bulk resistivity of the soil can be calculated

172 according to Ohm's law:

$$\rho = K * \frac{\delta V}{I}, \tag{3}$$

173 where δV is the observed potential difference and I is the injected current. the primary concern is with the strength

174 of the received signal, rather than its phase relationship. A standard procedure is to use a pair of electrodes for

175 current injection and separate pair of electrodes to record the potential difference. After making multiple spatially

176 distributed measurements the recorded data is used to generate a tomographic image of the subsurface, in order to

177 determine the spatial distribution of soil electrical properties. These are interpreted in the context of a heterogeneous

178 subsurface structure. Inverse modelling is used to fit an earth model to the measured dataset. The inversion

179 procedure uses adjustments to the predicted model parameters to achieve convergence between the measured and

180 predicted datasets. A typical approach is to change the model until the misfit reaches a minimum. The model

181 is build upon a mesh (dimensionality is case dependent) which follows a pre-defined discretisation of the target

182 geometrical space and other constraints (e.g. limit values, smoothing factor, boundary conditions). The model cells

183 have corresponding cartesian coordinates and a parametric value associated, in this case a geoelectrical parameter

184 (e.g. resistivity, phase). Additional a-priori information about the environment (e.g. soil structure, temperature,

185 topography) will significantly improve the inversion result. However, inherent problems with geoelectrical inversion

186 are:

187 1. Non-linearity. The relation between parameters and data is often non-linear, therefore a linear approximation is

188 required to help solve the system of equations.

189 2. Solution stability. A small perturbation in the initial conditions can cause very different outcomes.

190   3. Non-uniqueness. Multiple models fit the data to the same degree of accuracy, hence choosing the "correct" model

191   is a challenge both conceptually and practically. These limitations of geoelectrical inversion apply to all geoelectrical

192   techniques that employ tomographic reconstruction of the data.

2.2.3   IP

194   In the absence of polarization, a sudden switch off of the current injected in the target medium should cause the

195   voltage between a pair of potential electrodes to drop from an initial value V_0 instantaneously to 0. However, if the

196   soil exhibits polarization, a gradual decay of the voltage can be observed over a finite time period, which is known

197   as the IP effect (Everett, 2013). In practice, this behaviour can be measured both in the time-domain and in the

198   frequency domain.

199   **Time-domain IP.** The acquisition principle here is technically similar to the one used for ERT. From the IP

200   recorded discharge curve we can obtain measurable quantities such as apparent polarizability η (Equation 4) or

201   partial chargeability m (Equation 5):

$$\eta = \frac{V(T)}{V_0}, \tag{4}$$

202   where V_t is the voltage measured at time T after current switch off.

$$m = \frac{1}{V_0} \int_{t1}^{t2} V(t)dt, \tag{5}$$

203   where $t1$ and $t2$ are the two limits of a time window during the voltage decay (Everett, 2013).

204   **Frequency domain IP.** FDIP is often referred to as SIP or EIS and uses a range of (typically discrete) frequencies

205   for current injection. The complex resistivity in both magnitude and phase is a function of the frequency of the

206   injected current signal. Polarization effects cause a phase shift between injected and recorded currents, therefore in

207   addition to ERT, FDIP method is able to measure the IP effect through its phase angle.

208   Empirical models such as Debye (Debye, 1929) or Cole-Cole (Equation 6) (Cole and Cole, 1941) have been developed

209   to describe the complex resistivity frequency dependence.

$$\rho^*(\omega) = \rho_0[1 - m(1 - \frac{1}{1 + (i\omega\tau_0)^c})], \tag{6}$$

210   Fitting the Cole-Cole model parameters to experimental data yields values for the chargeability m, relaxation

211   time τ_0 and frequency exponent c. It is worth mentioning this model can also be applied in the time-domain on

212   chargeability curves (Pelton et al., 1978) in order to extract corresponding parameters.

213   **EIT.** EIT is a method which uses the measurement principles of IP, and therefore used to determine complex

214   resistivity, but in addition incorporates a tomographic reconstruction capability, such as ERT (Zimmermann et al.,

215   2008). Therefore, EIT brings together information about the signal strength, shape and timing. Ultimately, it uses

216   the data to construct a tomographic distribution.

217   For soil research purposes the method is still in the incipient stages. It was successfully applied previously for

218   detecting electrical phase differences (Kelter et al., 2015), the low-polarizability of a water submerged root system

219   (Weigand and Kemna, 2017) and changes in polarization due to diurnal cycles and gradual nutrient deprivation

220   (Weigand and Kemna, 2018).

2.2.4   ECM

222   Chloupek (1972) found a direct correlation between root parameters, such as dry mass and surface area, and the EC

223   of root systems. The basic measurement procedure involves the connection of an LCR (Inductance-Capacitance-

224   Resistance) meter between an electrode attached to the base of the plant stem and another one inserted into the soil.

225   Previous studies established such correlations at a single measurement frequency (Dalton, 1995; Ellis et al., 2013)

226   or using a broader range of frequencies (Ozier-lafontaine and Bajazet, 2005). Primarily, the measured quantity for

227   ECM is still complex impedance. However, the impedance measurements are interpreted in terms of an analogue

228   electrical circuit. Dalton (1995) envisioned root segments as capacitor-resistance pairs connected in parallel. The

229   root segment capacitor has three components: xylem as an internal electrode, soil nutrient solution surrounding

230   the root as a second electrode and a poorly conducting plant tissue acting as a dielectric. Therefore, the complex

231   impedance can be expressed in terms of the equivalent root system capacitance C and resistance R as:

$$\hat{Z}^{-1} = \frac{1}{R} + i\omega C = \frac{1}{R} + i\omega \frac{\epsilon A}{4\pi r_2 ln(\frac{r_2}{r_1})}, \tag{7}$$

232   where ϵ is the dielectric constant, A is the geometrical surface area of the root tissue, r_1 and r_2 are the radius of

233   the inner root xylem channel and the root segment, respectively.

2.2.5   Relationship between geoelectrical methods

235   Considering what was previously enunciated, one may reach the conclusion that there is a certain degree of inter-

236   connectivity between all the geoelectrical methods. The main common denominator is the measurement of complex

237   electrical impedance, but different methods have different ways of mathematically expressing the recorded data,

238   such as the magnitude of complex impedance (ERT), polarizability and chargeability (IP) or electrical permittivity

239   (ECM). Secondly, methods differentiate by the type of current they use (DC or AC) or the domain they operate

240   in (time-domain or frequency-domain). In Figure 1 we formulated a summary diagram describing the relationship

241   between different methods and their corresponding measured quantities. This will potentially serve as an aid to

242   better understand how the geoelectrical methods were used to resolve parameters of the root zone in the studies we

243   review in the following section 3.

2.3   Translating geoelectrical measurement into root zone properties

245   It is important to note that geoelectrical methods do not quantify root zone properties directly. For this purpose an

246   additional calibration measurement is required to allow direct translation of electrical measurements into root zone

247   properties. This can be illustrated using the example of SWC. As mentioned, electrical measurements are sensitive

248 to changes in SWC, but the relationship is a function of multiple factors and no analytical expression is readily

249 available to describe it. Therefore, a dedicated method for estimating water content (e.g. TDR, neutron probe,

250 destructive sampling) is usually used in parallel to the geoelectrical method, in order to determine the dependency

251 of the electrical response on SWC variation by empirical means. The outcome of this exercise is a calibration curve,

252 which can subsequently be used to translate the geoelectrical measurements into SWC for the specific material and

253 under the specific circumstances. Unfortunately, a universal transfer function is unlikely to exist, due to the large

254 number of potential input factors, used to parametrize the root zone, such as porosity, saturation status or root

255 mass. Different calibration strategies have been adopted over the years. Earlier studies established simple linear

256 regression correlations between measured resistivity and SWC or root biomass, respectively (Michot et al., 2003

257 and Amato et al., 2008). However, the calibration process has recently become more systematic and new research

258 is looking into its simplification using deep learning prediction algorithms (Brillante et al., 2016).

2.3.1   Resolving pedological parameters

260 A more robust strategy involves the use of quantitative conceptual models to link electrical parameters and soil

261 properties (known as pedotransfer functions or PTFs). One of the first relationships of this kind described the

262 resistivity behavior of a brine- saturated sandstone in the context of borehole logging and was developed by Archie

263 (1942). However, Archie's law did not take into account surface conductivity, which becomes essential in samples

264 with an increased clay content. Based on Archie's relation, the Waxman-Smits (WS) model, established for shaly

265 sands, incorporates the presence of clay particles with surface conductivity effects (Waxman and Smits, 1968). More

266 comprehensive models have been developed based on both laws. The model proposed by Rhoades et al. (1989) relies

267 on the assumption of two separate electrical pathways, a continuous one through waterfilled macropores and a series

268 linked soil-liquid one. A model by Mualem and Friedman (1991) is based on the fact that the tortuosity factor

269 affecting the bulk electrical conductivity is identical to the one predicting hydraulic conductivity. Revil et al. (1998)

270 assumes surface conduction to be restricted to the part of the EDL where ions are adsorbed to the material surface

271 (Stern layer). The Linde et al. (2006) model takes into consideration the different behaviour of ions in the pore

272 space. The transport regime of anions is independent of salinity as opposed to that of cations, which have a different

273 regime for high and low salinity.

274 The decision over which model to apply is subjective for any given application, as more than one model may fit

275 the requirements. Laloy et al. (2011) compared existing pedotransfer models and suggested that the Linde model

276 performs better for a low resistivity regime (<100 Ohm.m), whilst WS performs better in the high resistivity regime.

277 As one can realize from early PTSs such as Archie's law, they were not initially intended for applications in the

278 root zone but for oil exploration. Therefore, the factors describing them are strictly pedological. In order to offer

279 a more comprehensive view of how geoelectrical methods can resolve root zone properties, the following subsection

280 briefly presents research efforts of describing the root electrical signature.

2.3.2   Resolving root system parameters

An electrical model developed by Dalton (1995) suggested that roots can be represented by a parallel resistance-capacitance (RC) circuit. More roots will imply more RC pairs connected in parallel. Therefore, the effective capacitance of a root system will depend on its structure and size. Ellis et al. (2013) concluded that capacitance was significantly related to root mass, length and surface area, but as a measurable quantity its predictive power is poor. They also obtained the best predictions for root length, which was significantly related to the ratio between capacitance and density. However, the Dalton model was tested and inconsistencies were found by both Ellis et al. (2013) and Dietrich et al. (2012), questioning the validity of a linear correlation between capacitance and root mass. Upon the removal of roots from a hydroponic solution it was realized that the capacitance of the solution was much higher than the capacitance of the root tissue. Arguably, the studies have shown that capacitance is correlated to root mass, but is not a direct means of measuring it.

Cao et al. (2010) also measured the electrical resistance of a root system submerged in a hydroponic solution. The resistance decreased with an increasing contact surface area of the root with the solution. These measurements contributed to the formulation of analogue circuits where the root system is realized as series of electrical resistors. Building on these results, Cao et al. (2011) used a spectrum of frequencies to analyse the elements of the root system analogue circuit. The study found that capacitance is a more useful parameter than resistance when it comes to root size estimation. Regression models were used in Amato et al. (2008, 2009) in order to link root mass density to resistivity measurements. The strong correlations led to the formulation of a logistic-growth model which later gave accurate predictions on field data acquired by Rossi et al. (2011).

3   Monitoring processes and resolving structure in the root zone

Geoelectrical methods are able to (1) monitor processes in near real time and (2) resolve structure, which is important for the study of soil-plant interactions because of the high significance of water content changes (Samouëlian et al., 2005) for these interactions and the presence of root organic matter (Amato et al., 2008) in the medium of investigation. Given that access to water plays a key role in plant survival, quantitative monitoring of water dynamics is helpful for defining the requirements and constraints, such as water availability, influx access points, transport parameters, flow pathways and for characterizing the environmental conditions, including soil texture, soil porosity, root characteristics, climate, geological setting and others. Detecting and quantifying root activity is crucial for understanding the extent of plant development and their reactions to stimuli (Mooney et al., 2012). Root architecture development is a visible indicator of the quality of the impact root system has on the plant's health and productivity, or on surrounding plants. The following subsections present an overview of the current state-of-play in geoelectrical monitoring research in three main application areas, namely (1) water dynamics (2) the detection of root organic matter and (3) the modelling of root zone processes.

313 3.1   Root zone water dynamics

314 Much geoelectrical research is focused on monitoring root water dynamics.a considerable body of literature focuses

315 on monitoring root water dynamics underlining its importance for soil studies.

316 3.1.1   Ex-situ studies

317 We examine studies performed ex-situ (in a laboratory environment), many of which were undertaken to try to illus-

318 trate the suitability of geoelectrical methods for monitoring solute transport in soils, or to determine soil properties

319 in a controlled experiment, which would not be possible on a larger scale. The majority of studies have adopted

320 a similar experimental set-up, whereby the soil volume of interest is surrounded by electrodes in order to enable

321 electrical current flow throughout the sample (Figure 2).

322

323 3.1.1.1   The signature of rootless soil

324   It is important to acknowledge that the studies mentioned here focus on the soil as a medium which does not

325 contain a root system, disregarding the effect such a system has on neighbouring physicochemical properties. The

326 existence of roots in soil adds a further layer of complexity to the geoelectrical attempt of monitoring hydrodynamic

327 processes. Therefore, we present an initiatory body of literature that aims to decipher the contribution of rootless

328 soil separately before expanding to applications which take roots into consideration.

329   Binley et al. (1996) used a dye staining experiment to show the ability of ERT to reconstruct flow pathways in

330 soil. Olsen et al. (1999) used ERT in conjunction with X-ray CT for the purpose of solute transport characterisation.

331 A rapid transport mode was detected through geoelectrical monitoring and was explained by the properties of the

332 macropore system detected by X-ray tomography. However, macropores could not be directly related to the electrical

333 tomogram because of the gap in spatial resolution, hence a causal link between the two observations could not be

334 established. Similarly to Binley et al. (1996), Koestel et al. (2007) demonstrated the benefits of using dye as a tracer

335 for electrical conductivity monitoring experiments. This was extended to a two-step tracer infiltration experiment

336 through a cylindrical soil column (Koestel et al., 2008), in which bulk electrical conductivity was translated to solute

337 concentrations. Figure 3 shows the evolution of concentration illustrating the ability of ERT to track the dynamics

338 of solute injection and transport at the laboratory scale. However, this type of observation was only possible when

339 a hydraulic steady-state existed and there was no spatial variation in the saturation states of the soil. Cassiani

340 et al. (2009) used SIP for the purpose of monitoring organic pollutants in soils, looking at DC and chargeability

341 responses from samples at different levels of water saturation obtained after the injection of air and a non-aqueous

342 phase liquid (NAPL). The study observed differences between the NAPL and air samples, which were attributed to

343 phase distributions across the samples and not to chemical interaction between solutes and surrounding liquid/solid

344 phases.

345 **3.1.1.2   The signature of the root zone**

346   By periodically irrigating a ginkgo tree, Wu et al. (2013) detected spatial and temporal variations in capacitance

347 with increasing water content. Also, the tomographic images provided visual representation of the process of

348 saturation and subsequent drying. Werban et al. (2008), in a pot experiment containing a Lupinus plant grown in

349 fine sand, set out to monitor spatial heterogeneity of water movement. Diurnal variations were found, which were

350 assumed to be a manifestation of RWU triggered by plant transpiration. Building on this, Garré et al. (2011) used

351 a 3D ERT to quantify water content changes in soil due to RWU and evapotranspiration. Resistivity variations

352 were correlated here with minirhizotron measurements of root development. Newill et al. (2014) demonstrated

353 the feasibility of using capacitive coupling insulated electrodes whose purpose is to reduce corrosion and avoid

354 polarization of the probes. The study presented a more efficient acquisition system for measuring impedance, which

355 resulted in the technique being able resolve water content fraction changes of up to 20%. However, it is important to

356 note that their study measured the magnitude of the complex impedance only, without consideration of polarization

357 effects.

358 **3.1.2   In-situ studies**

359 In an industrialized world with a rising demand for food in both quantity and quality, effective soil management for

360 agriculture is becoming increasingly critical. The majority of in-situ root studies have therefore focused on water

361 dynamics exhibited by agricultural crops. In this kind of setting it is difficult to separate the effect of rootless

362 soil as it was previously done for ex-situ studies. This underlines the necessity of laboratory trials that attempt

363 to understand and parametrize the more localized behavior of the root zone, which will subsequently support and

364 serve as reference for field trials.

365 One of the first studies that assessed the effectiveness of the ERT method in an agricultural context was by Panissod

366 et al. (2001). It revealed the existence of high resistivity patches under cover crops, and these patches were inferred

367 to be linked to plant water uptake. In the absence of appropriate pedotransfer functions, which create the link

368 between water content and electrical resistivity, the water distribution could not be estimated. Also, no ground

369 truth was available for comparison. The study was able to map anomalies in the resistivity distribution, thus

370 showing the potential of the ERT method, but the causal link between resistivity variation and water content

371 depletion remained an assumption. Michot et al. (2001) presented a more robust experimental design using TDR

372 measurements in parallel with ERT. Resistivity variations with time were observed under crops similar to the ones

373 identified by Panissod et al. (2001). Moreover, a wetting front was localized from the electrical tomogram and

374 preferential flow directions were identified. Michot et al. (2003) subsequently conducted a very similar field trial.

375 The resistivity-estimated water content was compared to that obtained from TDR. The %RMS (Root Mean Square)

376 error was less than 5 and the correlation factor around 0.8, which suggests good agreement between both techniques.

377 Consequently, the work proves the suitability of ERT to monitor soil available water reserves on the field scale.

378 One of the reference works for root zone water dynamics was presented by Srayeddin and Doussan (2009), who

379   conducted a field monitoring study of water uptake under sorghum and maize fields subjected to different watering

380   regimes. The study showed heterogeneous patterns of water depletion in the moderated and poorly irrigated fields.

381   Direct field water content measurements were used to calibrate the resistivity results. The water uptake was found

382   to have a quantitative (and not just qualitative) relationship with resistivity.

383   The field studies follow a similar experimental set-up to the studies mentioned in section 3.1.1. Figure 4 shows an

384   example of a typical survey arrangement on a linear profile. 2D resistivity images resulting from such an acquisition

385   scenario are presented in Figure 5. They demonstrate the extent to which ERT resolved the spatial distribution of

386   resistivity. Here, both the lateral and the vertical variability was likely caused by the plant water uptake.

387   Celano et al. (2011) compared two different soil management regimes, tillage and cover cropping, and found a

388   significant water reserve in the soil beneath the cover crops. The authors used laboratory derived calibration

389   curves between soil moisture and resistivity. The correlation coefficients between resistivity-estimated and directly

390   measured water content was found to be stronger than that observed by Srayeddin and Doussan (2009). However,

391   the latter measurements were carried out in situ, whereas the former ones were undertaken ex situ, which typically

392   requires additional experimental time and effort. All applications of geophysical monitoring represent a trade-off

393   between time, effort and data quality.

394   Nijland et al. (2010) presented a case study that used geoelectrical methods to quantify water availability in a

395   Mediterranean soil ecosystem. The study highlighted the power of the roots to penetrate the fractured bedrock

396   to reach water. Robinson et al. (2012) underlined the ease of use and convenience of data collection that an ERT

397   survey provides. They conducted a 3D survey to monitor moisture content in an oak-pine forest, which suggested

398   moisture stability in tree-covered areas and moisture instability in open areas. Beff et al. (2013) monitored WC

399   under a maize field through a joint assessment of ERT and TDR. The latter was used to achieve spatial coverage and

400   the former to achieve temporal coverage. The resistivity distributions reflected the maize row arrangements in the

401   field. Garré et al. (2013) monitored resistivity changes in mixed cropping systems showing a smaller depletion depth

402   for chili cultures compared to maize and Leucaena. Also, a higher depletion was detected close to the intercrop

403   hedges which implied a competition for water between different crop species. Garré et al. (2012) used semivariogram

404   interpretation of WC spatial distribution indicating moisture variability is highly influenced by soil heterogeneity.

405   Kelly et al. (2011) monitored water migration beneath crops. The resulting resistivity tomograms were compared

406   with WC values obtained using a capacitance probe. Moreover, the study recommended that ERT monitoring

407   should be integrated into irrigation programs.

408   ERT monitoring was also used by Musgrave and Binley (2011) to characterize the stratigraphy of a wetland

409   site. The 2D characterization with ERT was performed in combination with GPR. The study highlighted the

410   suppression of temporal changes in resistivity, which was explained by the occurrence of groundwater recharge,

411   providing a means of identifying such recharge areas.

3.2 Root structural and functional properties

3.2.1 Woody roots

3.2.1.1 Correlating root properties and geoelectrical measurements

Amato et al. (2008) and Rossi et al. (2011) found a strong positive correlation between resistivity measurements and root biomass. Rossi et al. (2011) also observed a dominating effect of the root biomass over other root zone properties, such as root length density (root length per unit volume), which raised the concern that this has to be taken into account by future studies to avoid bias.

In an in-situ experiment, Čermák et al. (2006) successfully estimated tree root absorption surface area with resistivity measurements. Also, the study showed a positive correlation between stem area and root absorption area. In addition, Mares et al. (2016) used ERT to capture the spatiotemporal variability in an active sapwood, which reflects the sapflow upscaling. Guyot et al. (2013) attempted to estimate sapwood area with the use of resistivity monitoring. However, the R^2 correlation between resistivity derived estimates and actual area was low. Jones et al. (2009) used ERT as a means of visualizing tree-induced subsidence. Leveling data indicating subsidence and ERT profiles were in agreement, both being influenced by climatic conditions. As the study did not include quantitative models to accompany and fit the resistivity datasets, the correlations are qualitative.

3.2.1.2 Mapping tree root systems

Mary et al. (2018) showed the potential of ERT and the Mise-á-la-masse (MALM) technique for mapping woody root system distribution in soil. The concept of MALM measurements is to inject electrical current into a conductive body and make surrounding measurements of voltage. Based on these measurements the extent of the body can be calculated. The assumption is made that the roots are the conductive body and that the current injected through the plant stem will eventually be passed into the subsoil through the root terminations (root hairs). Another study by Zenone et al. (2008) combined ERT reconstruction and GPR sections for the purpose of root detection. Figure 6 shows the level of performance that can be expected from ERT when imaging root architecture. The root system is not resolved accurately, but the potential to localize roots is undeniable and the overall shape of the root system is captured well. The study also concluded that combining electrical resistivity with GPR data is useful in the investigation of root shape and behavior. It was shown that the contemporaneous use of multiple geophysical methods improves the quality of the results. GPR was successful for identifying the distribution of the roots in the subsoil, whereas ERT was useful for estimating the root volumes. Leucci (2010) used ERT, GPR and seismic refraction to produce 3D images of tree-root distribution. GPR revealed the extent of the root system, seismic refraction delineated the subsurface layers and ERT distinguished the roots from an old pipe system. The study reinforced the utility of the methods for this application emphasized the benefits of combining the techniques.

3.2.1.3 Root polarization

Zanetti et al. (2011) observed the complex conductivity signature of multiple samples of dead roots in three different soil textural environments dominated by gravel, sand and silt, respectively. Additionally, the methodology

446   was able to indicate the presence, type, size and orientation of buried material. However, measurements were limited

447   to 1D, hence no information about the spatial distribution of the buried samples could be obtained. Polarization

448   effects have also been observed by Martin (2012) when studying wood, suggesting that the methodology was able

449   to identify infection damage in wood cells, which could add significant value to the technique.

450   Mary et al. (2016, 2017) demonstrated the feasibility of using IP for root detection, whilst performing in-situ

451   experiments. Mary et al. (2016) concluded that a dry soil medium is more appropriate for IP measurements as

452   the contrast between the response from roots and surrounding soil is higher. Mary et al. (2017) concluded that, at

453   low frequencies (1 Hz chosen as adequate), significant effects of polarization are dependent on root per soil volume

454   ratio and are sensitive to root orientation. Furthermore, Mary et al. (2017) suggests root WC is proportional to

455   the amplitude of polarization. These results suggest that there is an increasing prospect of using this method in

456   the study of soil-plant interactions.

457   3.2.2   Herbaceous roots

458   Aulen and Shipley (2012) identified a significant relationship between root mass and capacitance. Unfortunately

459   this was too weak without prior species specific calibrations ($R^2 = 0.3$). Ellis et al. (2013) confirmed a weak

460   predictive power of ECM ($R^2 = 0.21 - 0.31$), but suggest an empirical model as a reasonable predictor of root

461   length ($R^2 = 0.56$). Amato et al. (2009) tested the ability of resistivity tomography to detect low-density root

462   systems. They concluded that, although promising for more developed root systems, the resistivity contrast is not

463   sufficient for a low-density regime.

464   Sabo et al. (2016a,b) proposed the use of capacitance tomography to assess the difference between healthy and dead

465   roots by their ability to absorb water containing nano-particles of iron. Healthy roots showed capacitive readings

466   that were up to three times lower than diseased ones. A series of pot experiments demonstrated the capability of

467   capacitance measurements to monitor root system properties (e.g. dimensions, mass, root surface) when subjected

468   to herbicide aceochlor (Cseresnyés et al., 2012), mycorrhizal fungal colonization (Cseresnyés et al., 2013), different

469   RWU rates (Cseresnyés et al., 2014; Cseresnyés et al., 2016) and SWC changes together with mycorrhizal activity

470   under field conditions (Cseresnyés et al., 2018). The latter study concluded that EC dependency on SWC is plant

471   species dependent, which underlines the importance of root system architecture through its impact on RWU rate of

472   change. Weigand and Kemna (2017) applied EIT to monitor the root activity of oil seed plants, which were grown

473   in hydroponic conditions. The study discovered a low-frequency polarization response associated to root presence,

474   and the methodology was able to delineate the extension of the root system. The study also observed changes in

475   electrical properties due to root physiological stress imposed by nutrient deprivation.

476   3.3   Root zone conceptual models

477   Root zone processes and structure are vastly complex. Formulating both conceptual and quantitative models of the

478   root zone is important to help develop our understanding of their complexity. Improved root zone models may help

479 fulfill the long-term ambition to be able to predict future states of the soil-plant system. However, existing root

480 zone models are not universally valid and dependent on locally derived parameters, such as soil texture, porosity,

481 temperature fluctuations ,root mass and others.

482 Geoelectrical monitoring can help improve root zone modelling. As discussed in sections 3.1 and 3.2, geoelectrical

483 methods have demonstrated their capability to assess root water dynamics and root structure. The recorded

484 variation in electrical properties reflects root functions (e.g. water uptake) or root-system structural indicators (e.g.

485 mass, length, density). In this section we discuss how this information was in turn used as a basis for models of

486 the root zone in order to 1. estimate the water balance determined by the soil-vegetation interaction 2. estimate

487 effective water uptake in order to optimize irrigation practices and 3. improve conversion between electrical data

488 and crop-scale root zone parametrization. A list of cited articles and corresponding models used can be found in

489 supplementary materials (Appendix A and B).

490 ### 3.3.1 Modelling root zone water dynamics

491 **3.3.1.1 Interaction between vegetation cover and soil water balance**

492 Cassiani et al. (2012) used ERT in conjunction with EMI method and TDR to investigate the effect of vegetation

493 upon water dynamics. A strong correlation was found between the presence of vegetation and the variability of

494 SWC. It was suggested that spontaneously grown vegetation on the bare soil influences the degree of soil compaction,

495 which led to a slow infiltration of meteoric water in the upper layers. This is one of the few studies that have at-

496 tempted to model vegetation-soil interaction based on electrical monitoring data. This approach holds promise for

497 future research and opens the door for more comprehensive modelling which should take into account the dynamics

498 of vegetation growth. Michot et al. (2003) demonstrated the effectiveness of combining ERT and TDR, in 2D some

499 10 years prior, but Cassiani et al. (2012) undertook 3D reconstruction of SWC distribution. Whilst geoelectrical

500 methods alone are capable of providing time-lapse information, TDR can be useful for its superior temporal res-

501 olution. It is also worth noting ERT systems with permanently deployed sensor arrays and instrumentation are

502 actively being developed, providing superior repeatability and high temporal resolution from ERT measurements

503 alone (Chambers et al., 2014).

504 Boaga et al. (2014) used ERT to demonstrate flooded plants are able to create aerated layers below the flooded

505 surface when transpiration rate was high. The study found the results were in agreement with the model previously

506 developed by Tosatto et al. (2009), which solved the 2D two-phase flow equations in porous media. Ursino et al.

507 (2014) showed that in fallow plots infiltration is heterogeneous, water redistribution takes place below ground where

508 roots have access to the active volume and the root-soil interplay reduces runoff and increases evapotranspiration.

509 Their study promoted the integration of measurements of soil properties such as electrical resistivity, moisture con-

510 tent and vegetation density in order to develop a comprehensive soil-plant interaction model. However, the study

511 did not employ a meaningful quantitative translation between electrical measurements and soil properties.

512 **3.3.1.2   Contributing towards irrigation efficiency**

513   Boaga et al. (2013) used ERT for temporal monitoring in order to characterize water balance exchanges in the

514 subsoil under an apple orchard. Root growth was closely connected to the geometry of the irrigation system as roots

515 developed in a shallow area, and were aligned with the irrigation lines. Cassiani et al. (2016) built on this approach

516 by developing a model of the unsaturated zone flow using 3D Richard's equations. This revealed the potential of

517 the method for monitoring and possibly predicting the time at which fresh irrigated water replaced saline water

518 already present in the soil.

519 Cassiani et al. (2015) used a 3D ERT system to monitor the root zone of an orange tree. Other measurements of sap

520 flow, eddy covariance and evapotranspiration were used in combination to develop a 1D model based on Richard's

521 equation, which described the water dynamics of the monitored soil volume. This calibration was successful and

522 predicted a much smaller water volume than the resistivity derived estimation. The implication was that over

523 50 % of irrigated water was not taken up by plants, illustrating the importance of quantitative modelling to help

524 interpret electrical monitoring data. Furthermore, Consoli et al. (2017) monitored and compared the impact of

525 full versus partial irrigation, based on a reduction of water input by 50%. The study showed that water efficiency

526 and fruit yield increased when a partial irrigation regime was used, which also implied that overirrigation affected

527 productivity.

528 **3.3.1.3   Enhancing the pedotransfer calibration**

529   In an effort to avoid site-specific calibrations and to make the irrigation process more efficient, Brillante et al.

530 (2014) developed a pedotransfer function to estimate WC from ER data. The function is obtained through the use

531 of a learning algorithm and estimated soil water wetness. It performed moderately well, showing a correlation of

532 0.67 between measured values and resistivity derived estimates of WC. Nonetheless, the methodology holds promise

533 due to its potential to reduce laboratory effort to calibrate the resistivity results.

534 Moreno et al. (2015) used a model of water flow and solute transport to differentiate between the contribution

535 of state variables (WC and salinity) to resistivity. Other studies discussed above have focused on plant inputs

536 (Cassiani et al., 2015; Ursino et al., 2014), whereas their study was aimed at improving the quantification of

537 non-plant related inputs to bulk resistance values. Both approaches are necessary in future modelling efforts.

538 Plant physiological measurements were combined with ERT measurements by Brillante et al. (2016), in a study of

539 grapevine. The work revealed that variability in the water uptake regimes was highly dependent on plant water

540 stress as striking differences between regimes during night and day were found. Brillante (2016) fitted two models

541 to predict soil water variation with the aid of field measurements of electrical resistivity. Instead of using absolute

542 values of electrical resistivity for model fitting, this study used their variations as predictors. They also used several

543 machine-learning techniques to tune the model parameters in order to avoid over-fitting. For the current datasets,

544 the gradient boosting machine method outperformed the others. Finally, the model results were compared to TDR

545 measurements reaching to a satisfactory agreement (RMSE 22.6%).

3.4 Other applications

3.4.1 Resolving pedological parameters

Morari et al. (2009) combined resistivity imaging, EMI and geostatistics and concluded that conductivity correlated positively with coarser textural soil components and negatively with finer components. Furthermore, this approach served as a basis for mapping subregions of the field within which crops are similarly affected by seasonal differences in weather and soil management. Celano et al. (2010) conducted a survey with the aim of establishing a correlation between pedological parameters, calculated through field sampling measurements, and electrical resistivity measurements. As resistivity measurements are sensitive to differences in salinity, ERT proved efficient in detecting salt accumulation in soil. Electrical monitoring was used to distinguish between different tillage systems in Basso et al. (2010). Soil properties such as bulk density or water storage are affected by tillage, therefore resistivity profiles showed significant differences between the soil practices. Future studies on this subject should consider correlating the variation in the electrical response with soil structure appraised by higher resolution imaging methods (e.g. X-ray CT). Kowalczyk et al. (2015) attempted to identify peat horizons through application of ERT, however, the heterogeneity of the soil made the inversion results inconclusive. The inversion generalized the resistivity values associated with the organic layers and treated them as parts of a sand layer, a result confirmed by a forward model based on geological units determined by drilling. It would seem that, identifying soil peat horizons in this manner is currently below the ability of the ERT method alone due to the length scales involved.

3.4.2 Plant phenotyping

Plant phenotyping is an emerging research area concerned with quantitative measurement of the structural and functional properties of plants. Lu et al. (2018) compared root zeta potential for 17 types of crops using streaming potential measurements whereby an electrical potential is generated when an electrolyte passes through a porous plug with charged surfaces. The study only found distinctive differences between legumes and non-legumes, due to a higher concentration of functional groups in the former. Combined ERT and EMI measurements were used to phenotype roots in the field by Whalley et al. (2017). The result of their study suggested that by comparing the shifts in patterns of soil moisture content, genotypes may be differentiated. Genotypic differences, more obvious in dry conditions, were observed in depth of water uptake and in the extent of surface drying. This result is very important for the economics of agricultural practices as the geophysical approach potentially saves time and effort spent on root excavation for direct measurements. The effect of soil physicochemical properties on the discrimination power of this method has yet to be investigated. Therefore, the first step is to test the phenotype discrimination methodology under different agropedoclimatic conditions and subsequently verify which factors enhance or diminish it.

4   Discussion and future outlook

4.1   Geoelectrical methodology and capabilities

4.1.1   Choice of geoelectrical method

The majority of geoelectrical methods are concerned with measurements of electrical impedance (Section 2.3). The main distinction between the nature and complexity of information resides in the information extracted from such measurements. Firstly, we can distinguish between single-frequency and multi-frequency acquisition strategies. Multi-frequency measurements offer additional information about polarization processes, but extracting electrical parameters, such as chargeability or relaxation time across a frequency spectrum is not straightforward and requires more acquisition time. However, methodology (Weigand and Kemna, 2017), instrumentation (Zimmermann et al., 2008) and sampling strategies (Weigand and Kemna, 2016) associated with spectral methods are rapidly developing and are likely to replace the more extensively used single-frequency or DC methods, such as ERT, for root zone monitoring applications.

One of the overarching themes of this review is root detection. There is clear evidence for a strong correlation between the imaginary resistivity component and root parameters (Chloupek et al., 1972; Ellis et al., 2013; Weigand and Kemna, 2017), but several studies have also found a correlation between the real part and root parameters (Cermak et al., 2006; Amato et al., 2008; Rossi et al., 2011). However, electrical resistivity was only correlated to root biomass and failed to reflect other root physical parameters such as root length density. In addition, resistivity studies showed greatest success when investigating woody roots, and further studies indicated that the resistivity contrast generated by low-density herbaceous roots is indistinguishable from the effect of other root zone features such as WC or grain size (Rossi et al., 2011). Furthermore, methods that include measurements of polarization have the potential of resolving not only root physical parameters, but characteristics of root activity such as interactions with fungi colonies (Cseresnyés et al., 2013) and reaction to physiological stress (Weigand and Kemna, 2017) or even root health (Sabo et al., 2016a). In summary, measurements of imaginary impedance have proven more conclusive for root investigation and offer a broader range of applications.

Figure 7 shows the increase in research articles featuring geoelectrical applications in the root zone, which highlights the rising interest in the use of such methods. It also shows that the use of classical ERT is in decline compared with other methods, whereas the use of ECM and SIP is growing. In addition, our analysis shows that the number of laboratory studies in this area has grown over time. This clearly reflects the increased effort dedicated to method development, especially for advance geoelectrical methods beyond ERT. These tend to require significantly more sophisticated instrumentation and greater care to obtain good quality measurements. So far they have therefore mostly been employed ex-situ, although field applications are likely to increase once the methodology development has reached a greater level of maturity.

4.1.2   Acquisition set-up and inversion algorithm

The dimensionality aspect of geoelectrical investigation is not to be treated lightly in the context of root zone monitoring. Previous research makes a clear distinction between the appraisal of a finer discretized model monitoring a singular root system, usually at lysimeter scale, and coarser models, usually at field scale. In addition, field surveys obtain a 3D properties distribution either by collating multiple 2D acquisition lines of superficial electrodes (Leucci, 2010) or by using a square array of acquisition with borehole electrodes (Cassiani et al., 2016). Using just one acquisition line, for 2D surveys, implies an easier set-up and quicker repetitive measurements. However, an agriculture field-site displays spatial heterogeneity, which this type of set-up fails to capture. A 3D survey by multiple superficial electrodes will provide the data coverage required, but will imply an expense in resolution. In contrast, using borehole electrodes allows higher resolution (especially in depth) but limits the user to a confined field sub-volume of investigation (1-2 m^3).

We mentioned previosly (section 2.3) that the tomographic model mesh of the subsurface is discretized according to the specific volume of investigation. However, the inversion problem becomes increasingly delicate when one attempts to obtain a model of the root zone. Firstly, there is a question of scale which closely matches the aquisition options described above. A lower resolution survey (depending on electrode arrangement) will imply coarser mesh discretization. Secondly, there is a question of electrical property variability. The root, rootles soil and the volume surrounding their interface (i.e. the rhizosphere) can be considered as electrically distinct areas, which in consequence can be constrained differently. As we have demonstrated, knowledge about each of these areas exists individually. However, the challenge for future research is to collate this information into one electrical model and further refine inversion strategies around this parametrization. For example, providing one has information about the extent of the root system, this volume can be also meshed, disconnected and assigned a different smoothing factor from the rest of the surrounding soil.

4.1.3   Electrical response from woody versus herbaceous roots

The two categories of roots display different electrical responses. Essentially, the difference in size, not the root functionality, appears to account for the distinction. The larger woody root, with a higher density and surface area, showed higher correlations with electrical resistivity and had a bigger impact on its change than finer roots found in the same system (Rossi et al., 2011). In terms of polarization, other soil properties, such as WC, are important in order to obtain a good response (Mary et al., 2016,2017). Furthermore, both types of roots show polarization, but not necessarily at the same frequencies. Weigand and Kemna (2017) reported a strong polarization at 70 Hz for herbaceous roots and Mary et al. (2017) reported 1 Hz to be suitable for woody roots. The distinct polarization frequencies could prove to be important for root classification if future research considers the analysis of larger scale root systems, which contain both kinds of roots.

641 ## 4.2   Knowledge gaps in pedophysical relationships

642   It is a common observation in the literature that none of the previously developed pedophysical relationships

643   (pedotransfer functions for geoelectrical data) is perfectly adapted to the specific site conditions (e.g. soil texture,

644   porosity, organic matter content) under investigation (Laloy et al., 2011). Therefore, calibration is usually required

645   in order to empirically determine new functional parameters corresponding to each individual site.

646   ### 4.2.1   Formulating pedophysical relationships in the lab

647   When considering a rootless soil calibration, most of the studies that have employed pedophysical calibration for field

648   measurements have used soil samples repacked ex-situ. It is extremely difficult to recreate the chemical composition

649   of the pore water (Furman et al., 2013) and a sample's natural pore structure under laboratory conditions. Working

650   with disturbed samples disregards the effect of pore tortuosity, considered essential when evaluating conductivity

651   pathways and consequently bulk resistivity measurements (Rhoades et al., 1989). Also, agricultural soils are quite

652   frequently subjected to anthropic interactions, which generate spatial and temporal variations which can effect

653   soil compaction. The latter is known to be a direct control on resistivity (Romero-Ruiz et al., 2018). In these

654   circumstances a well suited approach is performing calibration measurements on undisturbed soil samples or to be

655   attempted in-situ (Srayeddin and Doussan, 2009; Michot et al., 2003).

656   We previously mentioned (section 2.2 and 3.1.1) the distinction some of the studies make between analysing electrical

657   properties of the rootless soil, the root system or the root zone as a whole. We consider each has its own merit and

658   corresponding relationships between root zone properties and electrical parameters important for future research.

659   Currently, many studies referenced in our review (Srayedin and Doussan, 2009; Celano et al., 2011; Garré et al.,

660   2013) are interested in the observation of root activity (e.g. suction), therefore being able to translate electrical

661   measurements to WC balance of the target volume is crucial. In this case one would not be able to depict the

662   outline of root system itself, but only deliniate the impact on the surrounding soil. However, one can expand this

663   methodology and determine root suction variability under different climatic, nutrient availability or soil textural

664   conditions. This will contribute to our knowledge of plant health and yield potential. Also, plant phenotyping

665   represents a promising potential application of geoelectrical research as suggested (Whalley et al., 2017). However,

666   the methodology needs to be proven suitable in different environements before its effectiveness can be demonstrated.

667   Furthermore, one may be interested in quantifying root development, therefore firstly would require the derivation

668   of a clear electrical response from the rootless soil. Any variation from the base electrical spectrum would imply root

669   mass development or root activity. The rate of development obtained as such could determine a plant's medium

670   adaptability or its interaction with other elecments of the ecosystem.

671   ### 4.2.2   On the variability of pedophysical relationships

672   Garré et al. (2011) underlined the necessity for horizon-specific calibrations for an undisturbed soil column. Also,

673   Furman et al. (2013) acknowledged climate seasonal variations in climate cause not only changes in WC, but also salt

674 accumulations, thus making concentration of solutes in the water-filled pore spaces variable with time. Ultimately,

675 for an accurate description of soil properties it is desirable to include high spatial and seasonal temporal variability.

676 We have mentioned above the effect of roots on bulk resistivity measurements, which is caused by the electrically

677 conductive pathways they form (created by the nutrient solution absorbed through the xylem) and EDLs both at

678 the exterior and interior surfaces of the root. The literature offers examples of empirical relationships between root

679 biomass and resistivity (Amato et al., 2008), therefore we recommend future studies should include this aspect

680 in the formulation of pedotransfer functions. Also, root system development alters the soil structure and its

681 chemical properties, invariably changing the electrical properties of the surrounding soil. Future research should

682 therefore consider combining existing numerical simulations of root architecture and its impact on soil hydraulic

683 properties (Postma et al., 2017) with geoelectrical numerical models in order to achieve a more realistic pedophysical

684 calibration.

685 ### 4.2.3   Computational approaches in pedophysical calibration

686 A different way of approaching the translation is emerging from the field of data science, including 'big data' analytics

687 and parameter prediction methods based on machine learning. Rather than attempting to develop a universal

688 analytical transfer function, a more adequate result might be obtained by calculating an 'educated estimate' based

689 on prior knowledge from existing data. Provided a sufficiently large input dataset exists, deep learning algorithms

690 can be utilized to predict an effective representation of the desired output parameter. Examples of work in this

691 direction have already appeared in the literature (Brillante, 2016). An emerging trend in data science is convolutional

692 neural networks (Pound et al., 2017). These computational systems, inspired by natural neuronal architectures,

693 have the capability of developing a learned strategy that extracts the relevant characteristics from an existing

694 series of inputs. When presented with a new input, the neural networks are able to identify in the new input

695 the characteristics previously learned (based on the learned model) and subsequently classify or make a prediction

696 from it. These kinds of algorithms are now widely used in image processing and pattern recognition. In soil

697 science applications, a neural network could be used to predict moisture content, provided it was 'trained' with a

698 large enough dataset containing other soil parameters including electrical data. Future opportunities will lie in the

699 potential of such networks to transfer between domains. This implies that a network trained on a wide range of

700 different experimental conditions could capture a more general model of the transformation which in turn could be

701 tuned to new conditions by additional training with a comparatively small amount of data. Attempts to use such

702 networks in soil and rock physics have already been reported in the literature (e.g. Pachevski and Timlin, 1996;

703 Koekkoek and Booltink, 1999). Also, different machine learning methods are already being employed in an effort

704 to enhance the fit between models of soil water balance and electrical resistivity data (Brillante, 2016).

4.3 Enhancing the geoelectrical characterization of the root zone

The tomographic imaging capability of geoelectrical methods offers unique quantitative information about the spatial variability of soil properties. Especially for field investigations it is desirable to be able to obtain large scale images of the subsurface. However, geophysical inversion is ill-posed and requires regularization, ideally combined with additional (a-priori) information in order to create an accurate model of the subsurface. The constraints are often unsatisfactory when inversion is applied to geoelectrical data alone. In this section we discuss strategies to reduce the uncertainty in the geoelectrical images.

4.3.1 Use of complementary datasets

In Section 3.1 and 3.2 we have discussed studies that simultaneously employed ERT together with other electromagnetic methods for synergetic monitoring and characterization of soil moisture. Complementary techniques include TDR (Beff et al., 2013, Boaga et al., 2013, Michot et al., 2003) GPR (Musgrave and Binley, 2011; Leucci, 2010) or EMI (Cassiani et al., 2012; Morari et al., 2009; Whalley et al., 2017).

The most commonly used method that provides complementary data is TDR. It measures the dielectric permittivity of the soil which is subsequently converted into SWC (Topp et al., 1980). TDR probes position usually follows the electrode arrangement used for geoelectrical surveying (Figure 2). This offers the advantage of directly comparing results without the need for correction for spatial distribution, scale or mesh discretization. Therefore, in the context of geoelectrical research, TDR data is mainly used for ground truth and can help isolate the contribution of SWC to the bulk resistivity response. Given the prevalence of TDR measurements in the literature, it could easily be assumed that TDR is sufficient for monitoring soil moisture variability. However, whilst TDR does provide good temporal resolution, is restricted to single point measurements, and therefore offers only limited spatial coverage. In contrast to TDR, the output of GPR and EMI is an image of the subsurface, therefore they generally provide good spatial coverage. GPR offers a high spatial resolution and is primarily used to delineate zones with different lithology. Due to the physics of low frequency electrical flow, it is difficult to obtain sharp lothological boundaries (including soil horizons) from ERT images (e.g. Figure 5), but GPR data has the potential to enhance this (Musgrave and Binley, 2011). Due to the nature of the instrumentation, EMI provides a very fast and effective way of determining the spatial distribution of soil electrical conductivity and resolving lateral contrasts on a large (field-) scale. However, EMI is faced with intrinsic challenges such as the lack of vertical resolution. When combined with ERT, it is possible to obtain comprehensive field-scale models of conductivity variation both laterally and vertically. Joint interpretation of this kind has proved successful for aquifer characterization (Linde et al., 2006) or estimating field scale soil hydraulic conductivity (Farzamian et al., 2015). Previous authors have highlighted the capabilities of a combination of EMI and ERT for root zone imaging and soil moisture characterization (al Hagrey, 2007).

Other complementary methods involve measuring soil parameters destructively. A number of studies presented in this review (Amato et al., 2008; Rossi et al., 2011; Celano et al., 2010; Zenone et al., 2008) quantified root length density (RLD) or root biomass (RMD) by collecting all the roots in the analysed sample and measuring their length

739   and weight, before correlating this information to electrical results. This procedure is perhaps useful for proof

740   of concept, but a fully non-invasive strategy is clearly more desirable for practical applications, particularly for

741   monitoring processes in the root zone over time.

4.3.2   A-priori information about the root zone

743   Soil structural details are an example of the kind of highly relevant additional information required and represent

744   a good source of a-priori knowledge. Alternative methods of tomographic imaging from other fields of science are

745   well developed, including X-ray CT, MRI or neutron imaging. These are able to provide details of soil structure at

746   high resolution (down to 1 μm. There is significant future research potential in conducting joint experiments that

747   include the synergetic application of geoelectrical methods and high-resolution structural imaging methods, both

748   appraising the same soil volume. Early attempts were made by Olsen et al. (1999) and Cassiani et al. (2009) using

749   X-ray information to explain patterns in the electrical response, but conclusions were qualitative and a quantitative

750   link is currently missing. Three-dimensional reconstruction of the pore architecture to a high resolution allows the

751   calculation of pore network parameters (e.g. pore diameter, connectivity). On this basis, subvolumes of the pore

752   space that account for fluid percolation in the soil sample can be identified (Koestel et al., 2018). This information

753   can in turn be used to constrain geoelectrical inversion results, e.g. by specifying regions of the soil volume with an

754   increased or decreased propensity to fluid movement. Those regions are likely to be associated with greater changes

755   in electrical properties.

756   X-ray CT is also a very effective ground-truth method for root characterization as it permits reconstruction of

757   the root system to a high spatial resolution by segmenting radiograms of the root zone (Mairhofer et al., 2016).

758   This kind of information can be parametrized accordingly and included into coupled frameworks containing both 3D

759   electrical and root architectural data. As previous laboratory polarization studies have looked at roots in hydroponic

760   solutions (Cao et al., 2010; Weigand et al., 2017,2018) this strategy can serve to develop our understanding of root

761   electrical properties in soils. The exact spatial position of every root segment can be used to modify the finite

762   element mesh of the starting model for the geoelectrical inversion. We have highlighted studies that represent the

763   root system as an electrical circuit analogue (Dalton et. al, ; Cao et al., 2011); in that context the root segment

764   contribution to electrical properties can be quantified. Subsequently this contribution can be associated with the

765   corresponding mesh element and its impact on the electrical inversion results assessed (Rao et al., 2018). Given

766   that previous research has established that preferential infiltration can happen along main root channels (Werban

767   et al., 2008), it is therefore possible to quantify the contribution of individual root segments to water uptake using

768   suitable parametrization in the geoelectrical model.

4.4   Enhancing root zone conceptualisation

770   Various authors have suggested conceptual models for the root zone, including models (complete list in Appendix

771   B) that represents root materials as resistors (Cao et al. 2010; Ellis et al. 2013), models which account for water

772 movement (Cassiani et al. 2016; Ursino et al. 2014) or a model that accounts for both, biomass and soil moisture

773 (Cassiani et al., 2012). In this section we will discuss the current state of conceptualization of the root zone and

774 propose future research opportunities from a geoelectrical perspective.

4.4.1 Root analogue electrical circuit models

776 According to Ozier-lafontaine and Bajazet (2005), the root zone system can be electrically divided into multiple

777 components, namely the stem-root internal medium, the soil-root interface, the soil medium and the electrode con-

778 tact with the plant/soil. Every component has a different manifestation with respect to conduction and polarization.

779 Each requires careful electrical parametrization and their contribution to the overall electrical response needs to be

780 appropriately quantified. For example, currently there is no clear distinction between the contributions from the

781 root mass and the root-soil interface to capacitance measurements.

782 The Dalton model is considered an important benchmark for the way the root system is electrically represented, as

783 multiple groups of Resistance-Capacitance (RC) pairs connected in parallel. However, inconsistencies in the Dalton

784 model have been reported (Dietrich et al., 2012; Ellis et al., 2013), forcing a rethink in the way the soil-root system

785 is electrically interpreted. One can regard the Dalton model as an oversimplified analogue, and in fact a more

786 comprehensive model includes a combination of series and parallel RC groups Cao et al. (2010). Furthermore, for

787 hydroponic systems, both Dietrich et al. (2012) and Cao et al. (2010) suggest that the root tissue above the solution

788 surface is the main contributor to capacitance and resistance. The analogue circuit model architecture and relative

789 contribution of individual components are key concepts that will guide the future quest for more effective models

790 of the root zone.

4.4.2 Separating contributors to the electrical response

792 Recent studies have attempted to develop models which simulate the soil system water balance and use them as

793 a substitute for collecting field data, highlighting the effectiveness of an accurate model (Cassiani et al., 2012).

794 Frequently, soil electrical conductivity changes are solely attributed to variations in WC, but in fact multiple con-

795 tributors can be responsible, including levels of salinity or organic content and distribution. Therefore, quantitative

796 models require a clear separation between such contributors when computing electrical conductivity. It is also im-

797 portant that model boundaries take into account the open nature of the system being studied, as energy and mass

798 are exchangeable with the medium surrounding the modeled system. Many models lack robustness from the poor

799 definition of boundary fluxes (Garré et al., 2011). Therefore, better mathematical expressions of such exchanges

800 are required, reflecting evapotranspiration, rain water influx, groundwater movement and others.

801 Future laboratory studies should firstly focus on the rootless electrical response to water content variation and

802 only secondly introduce roots into the system once the medium is appropriately parametrized. Furthermore, the

803 presence of roots will undoubtedly change their surrounding medium. How much the different resulting elements,

804 such as: a modified soil structure, the suction power of root, mucilage formation or the presence of organic material

805 itself contribute to such change remains an unknown and must be explored.

806   4.4.3   Integrating plant hydrology models and geoelectrical measurements

807   The current state of computational technology allows the simulation and visualization of reasonably complex root

808   zone processes in four dimensions. Elucidating the impact of root architecture on root zone hydraulics is of increasing

809   interest especially for practical purposes, such as sustainable irrigation (Green et al., 2006). As different components

810   of the root system have different hydraulic properties (Javaux et al., 2013) the ability to simulate and quantify this

811   structural effect is essential for an accurate interpretation of monitoring root-water uptake. Access is already

812   available to models that can simulate root-growth for different plant types (e.g. CRootBox; Schnepf et al. (2017))

813   and even models that couple root growth with water or nutrient uptake simulations (e.g. OpenSimRoot; Figure

814   8). However, as underlined by Draye et al. (2010), it is still unknown if the soil or the plant is the main driver of

815   water flow, or indeed where the greatest barrier to water flow resides (e.g. root-soil interface, in the soil, in the

816   root). As geoelectrical data provide a proxy for imaging changes in WC, there is potential in developing a coupled

817   hydrological model of the root zone. From a plant research perspective, a useful review focused on plant biological

818   models across scales is given by Hill et al. (2013), who discusses the interplay between root biology and surrounding

819   soil system from cellular to crop level. The authors emphasize the need for monitoring quantitative changes in

820   root biology (e.g. hormones, water status, nutrients), a need that could potentially be fulfilled by geoelectrical

821   monitoring, as there is evidence that geoelectrical techniques are sensitive to root functional stress (Weigand and

822   Kemna, 2017). Hill et al. (2013) also argue for bridging the gap between genetic and environmental regulation. In

823   that context we believe that field scale geoelectrical surveys could provide an appropriate assessment of changes in

824   water dynamics, root activity or even root growth.

825   In the light of this, there is significant future research potential in developing a coupled multidisciplinary framework

826   for characterizing and monitoring root zone hydraulics (Figure 9). This framework comprises both a hydraulic and

827   an electrical model of the root zone. It will undertake forward simulations of root zone hydraulics and translate

828   the results to electrical properties via appropriate pedotransfer functions. The results will then be compared

829   with simulated electrical measurements acquired on the same soil volume. In Stage 1 we establish the baseline soil

830   medium and root network properties. This is followed by flow process modelling, expressing how does the properties

831   determined in the previous stage affect root nutrient/water uptake (Stage 2), mapping prior obtained parameters on

832   an appropriate mesh (Stage 3) and finally translating the model results into geoelectrical parameters (Stage 4). A

833   disagreement between both sets of results (measured and modelled geoelectrical parameters) would imply a shortfall

834   either in the way flow processes are implemented in the model or in the conversion between hydraulic and electrical

835   root zone properties (Figure 9 stage 2-3). The simulations could be iteratively repeated until the discrepancy is

836   minimized hence providing an opportunity to determine the value of unknown parameters which lead to the initial

837   misfit. This overall approach should allow us to simulate the electrical response in space and time holistically as

838   a function of both soil and root properties. At present, tools are available to conduct numerical simulations of

839   this kind at the individual plant scale, for example in laboratory containers under controlled conditions. Future

840   research could follow a similar strategy for field scale simulations, although there are other external effects such

841   as climate or vegetation growth (Cassiani et al., 2012), which need to be parametrized and integrated into the
842   modeling framework.

5   Conclusions

844   We sought to highlight the potential advantages and limitations that geoelectrical methodology can bring to re-
845   search in the soil sciences and in particular to root zone studies. Geoelectrical methods offer minimally invasive
846   data acquisition, are cost effective and have the ability to monitor key physical (soil water balance), chemical (soil
847   water salinity) and biological (root growth) processes in the root zone both in space and time. A body of literature
848   has developed, which shows these methods to be very effective for the examination of root zone water dynamics and
849   the detection and characterization of root architecture. We have presented and discussed the main characteristics of
850   both established and emerging geoelectrical methodologies. Currently, ERT is one of the best established and most
851   evolved techniques, however the information it delivers is limited to a single physical parameter and not without
852   ambiguity. ERT is by far the most frequently used technique in the literature, but other methods (e.g. SIP, TDIP,
853   EIT) provide more holistic measurements including electrical polarization. These have also proven their ability to
854   determine soil properties (albeit often under more controlled laboratory conditions), and can provide superior sen-
855   sitivity to root properties (e.g. mass, length), type (woody or herbaceous) and functions (e.g. evapotranspiration,
856   nutrient absorption). Future root zone research must therefore carefully consider the choice of geoelectrical method-
857   ology in experimental design. Particularly for larger scale root zone field studies the availability of techniques and
858   instrumentation is more limited.

859   Our evaluation of previous research has highlighted the difficulty of determining robust pedophysical relationships
860   (i.e. pedotransfer functions for geoelectrical data), which are required for meaningful property translation and
861   experimental calibration. We expect future research to take into account their variability in space and time and to
862   consider emerging trends in data science, including convolutional neural networks. Furthermore, due to the inherent
863   limitations in the spatial resolution of geoelectrical methods, we highlight the value of synergetic studies with other
864   soil assessment methods (e.g. TDR, EMI, GPR). Such a strategy is suitable for field scale characterizations of the
865   root zone and offers the potential of including high resolution soil and root structural information into geoelectrical
866   inversion models. Finally, we have demonstrated the benefits of geoelectrical information in root zone conceptual
867   modeling. We call for improvements to the analogue circuit representation of the root system components, under-
868   lining the need for separating the main contributors to the electrical property variations when constructing a model
869   and propose a coupled multi-disciplinary characterization and monitoring framework incorporating simulations of
870   plant growth-hydrological parameters and geoelectrical measurements.

871   These results underline the potential this methodology has to monitor and characterize vadoze zone hydraulic pro-
872   cesses. However, this study concerned rootless soil only, therefore the natural step forward would be to visualize and
873   appraise undisturbed soil volumes which contain roots. By monitoring how roots impact the hydraulic processes of
874   soil could offer new insights about root development, root health or even root-soil adaptability.

875 References

876 al Hagrey, A. S. (2007). Geophysical imaging of root-zone , trunk, and moisture heterogeneity. *Journal of Experimental Botany*,
877   58(4):839–854.

878 Alm, D., Cavelier, J., and Nobel, P. (1992). A finite-element model of radial and axial conductivities for individual roots - development
879   and validation for 2 desert succulents. *Annals of Botany*, 69:87–92.

880 Amato, M., Basso, B., Celano, G., Bitella, G., Morelli, G., and Rossi, R. (2008). In situ detection of tree root distribution and biomass
881   by multi-electrode resistivity imaging. *Tree Physiology*, 28(10):1441–1448.

882 Amato, M., Bitella, G., Rossi, R., Gómez, J. A., Lovelli, S., and Gomes, J. J. (2009). Multi-electrode 3D resistivity imaging of alfalfa
883   root zone. *European Journal of Agronomy*, 31(4):213–222.

884 Amin, M. H. G., Richards, K. S., Chorley, R. J., Gibbs, S. J., Carpenter, T. A., and Hall, L. D. (1996). Studies of soil-water transport
885   by MRI. *Magnetic Resonance Imaging*, 14(7-8):879–882.

886 Archie, G. (1942). The Electrical Resistivity Log as an Aid in Determining Some Reservoir Characteristics. *Transactions of the AIME*,
887   146(01):54–62.

888 Aulen, M. and Shipley, B. (2012). Non-destructive estimation of root mass using electrical capacitance on ten herbaceous species. *Plant*
889   *and Soil*, 355(1-2):41–49.

890 Banin, A. and Anderson, D. (1974). Effects of salt concentration during freezing on the unfrozen content of porous materials. *Water*
891   *Resources Research*, 10:124–128.

892 Basso, B., Amato, M., Bitella, G., Rossi, R., Kravchenko, A., Sartori, L., Carvahlo, L. M., and Gomes, J. (2010). Two-Dimensional
893   Spatial and Temporal Variation of Soil Physical Properties in Tillage Systems Using Electrical Resistivity Tomography. *Agronomy*
894   *journal*, 102:440–449.

895 Beff, L., Günther, T., Vandoorne, B., Couvreur, V., and Javaux, M. (2013). Three-dimensional monitoring of soil water content in a
896   maize field using Electrical Resistivity Tomography. *Hydrology and Earth System Sciences*, 17(2):595–609.

897 Binley, A. (1995). Regularised Image Reconstruction of Noisy Electrical Resistance Data. *Proceedings of the 4th Workshop of the*
898   *European Concerted Action on Process Tomography*, pages 401–410.

899 Binley, A. (2018a). *R2 software*. `http://www.es.lancs.ac.uk/people/amb/Freeware/R2/R2.htm` [Accessed: 18/01/2019].

900 Binley, A. (2018b). *R3 software*. `http://www.es.lancs.ac.uk/people/amb/Freeware/R3t/R3t.htm` [Accessed: 18/01/2019].

901 Binley, A., Shaw, B., and Henry-Poulter, S. (1996). Flow pathways in porous media : electrical resistance tomography and dye staining
902   image verification. *Measurement Science and Technology*, 7:384–390.

903 Boaga, J., D'Alpaos, A., Cassiani, G., Marani, M., and Putti, M. (2014). Plant-Soil interactions in salt marsh environments: Experi-
904   mental evidence from electrical resistivity tomography in the Venice Lagoon. *Geophysical Research Letters*, 41(17):6160–6166.

905 Boaga, J., Rossi, M., and Cassiani, G. (2013). Monitoring Soil-plant Interactions in an Apple Orchard Using 3D Electrical Resistivity
906   Tomography. *Procedia Environmental Sciences*, 19:394–402.

907 Brillante, L. (2016). Electrical imaging of soil water availability to grapevine : a benchmark experiment of several machine-learning
908   techniques. *Precision Agriculture*, 17:637–658.

909 Brillante, L., Bois, B., Lévêque, J., and Mathieu, O. (2016). Variations in soil-water use by grapevine according to plant water status
910   and soil physical-chemical characteristics-A 3D spatio-temporal analysis. *European Journal of Agronomy*, 77:122–135.

911   Brillante, L., Bois, B., Mathieu, O., Bichet, V., Michot, D., and Lévêque, J. (2014). Monitoring soil volume wetness in heterogeneous
912   soils by electrical resistivity . A field-based pedotransfer function. *Journal of Hydrology*, 516:56–66.

913   Cao, Y., Repo, T., Silvennoinen, R., Lehto, T., and Pelkonen, P. (2010). An appraisal of the electrical resistance method for assessing
914   root surface area. *Journal of Experimental Botany*, 61(9):2491–2497.

915   Cao, Y., Repo, T., Silvennoinen, R., Lehto, T., and Pelkonen, P. (2011). Analysis of the willow root system by electrical impedance
916   spectroscopy. *Journal of Experimental Botany*, 62(1):351–358.

917   Cassiani, G., Boaga, J., Rossi, M., Putti, M., Fadda, G., Majone, B., and Bellin, A. (2016). Soil-plant interaction monitoring: Small
918   scale example of an apple orchard in Trentino, North-Eastern Italy. *Science of the Total Environment*, 543:851–861.

919   Cassiani, G., Boaga, J., Vanella, D., Perri, M. T., and Consoli, S. (2015). Monitoring and modelling of soil-plant interactions: The joint
920   use of ERT, sap flow and eddy covariance data to characterize the volume of an orange tree root zone. *Hydrology and Earth System
921   Sciences*, 19(5):2213–2225.

922   Cassiani, G., Kemna, A., Cassiani, G., Kemna, A., Villa, A., and Zimmermann, E. (2009). Spectral induced polarization for the
923   characterization of free-phase hydrocarbon contamination of sediments with low clay content. *Near Surface Geophysics*, 7:547–562.

924   Cassiani, G., Ursino, N., Deiana, R., Vignoli, G., Boaga, J., Rossi, M., Perri, M. T., Blaschek, M., Duttmann, R., Meyer, S., Ludwig,
925   R., Soddu, A., Dietrich, P., and Werban, U. (2012). Noninvasive Monitoring of Soil Static Characteristics and Dynamic States: A
926   Case Study Highlighting Vegetation Effects on Agricultural Land. *Vadose Zone Journal*, 11(3).

927   Celano, G., Palese, A., Tuzio, A., Zuardi, D., L., L., and C., X. (2010). Geo-electrical survey on the soil of an apricot orchard grown
928   under semi-arid conditions. *Acta Horticulturae*, 862:425–428.

929   Celano, G., Palese, A. M., Ciucci, A., Martorella, E., Vignozzi, N., and Xiloyannis, C. (2011). Evaluation of soil water content in tilled
930   and cover-cropped olive orchards by the geoelectrical technique. *Geoderma*, 163(3-4):163–170.

931   Čermák, J., Ulrich, R., Staněk, Z., Koller, J., and Aubrecht, L. (2006). Electrical measurement of tree root absorbing surfaces by
932   the earth impedance method: 2. Verification based on allometric relationships and root severing experiments. *Tree Physiology*,
933   26(9):1113–1121.

934   Chambers, J. E., Gunn, D. A., Wilkinson, P. B., Meldrum, P. I., Haslam, E., Holyoake, S., Kirkham, M., Kuras, O., Merritt, A., and
935   Wragg, J. (2014). 4D electrical resistivity tomography monitoring of soil moisture dynamics in an operational railway embankment.
936   *Near Surface Geophysics*, 12(1):61–72.

937   Chloupek, O. (1972). The relationship between electric capacitance and some other parameters of plant roots. *Biologia Plantarum*,
938   14:227–230.

939   Cole, K. S. and Cole, R. H. (1941). Dispersion and Absorption in Dielectrics . *J. Chem. Phys.*, 9(1913):98–105.

940   Consoli, S., Stagno, F., Vanella, D., Boaga, J., Cassiani, G., and Roccuzzo, G. (2017). Partial root-zone drying irrigation in orange
941   orchards: Effects on water use and crop production characteristics. *European Journal of Agronomy*, 82:190–202.

942   Cseresnyés, I., Fekete, G., Végh, K. R., Székács, A., Mörtl, M., and Rajkai, K. (2012). Monitoring of herbicide effect in maize based on
943   electrical measurements. *International Agrophysics*, 26:243–247.

944   Cseresnyés, I., Szitár, K., Rajkai, K., Füzy, A., and Mikó, P. (2018). Application of Electrical Capacitance Method for Prediction of
945   Plant Root Mass and Activity in Field-Grown Crops. *Frontiers in Plant Science*, 9(February):1–11.

946   Cseresnyés, I., Takács, T., Végh, K. R., Anton, A., and Rajkai, K. (2013). European Journal of Soil Biology Electrical impedance and
947   capacitance method : A new approach for detection of functional aspects of arbuscular mycorrhizal colonization in maize. *European
948   Journal of Soil Biology*, 54:25–31.

949   Dalton, F. (1995). In-situ root extent measurements by electrical capacitance methods. *Plant and Soil*, 173:157–165.

950   Davidson, E. A., Belk, E., and Boone, R. D. (1998). Soil water content and temperature as independent or confounded factors controlling
951   soil respiration in a temperate mixed hardwood forest. *Global Change Biology*, 4(2):217–227.

952   Debye, P. (1929). Polar molecules. *New York:Chemical Catalogue Co.*, page 172.

953   Denmead, O. T. (1961). *Availability of soil water to plants.* Iowa State University.

954   Dietrich, R. C., Bengougha, A. G., Jones, H. G., and White, P. J. (2012). A new physical interpretation of plant-root capacitance.
955   *Journal of Experimental Botany*, 63:6149–6159.

956   Draye, X., Kim, Y., Lobet, G., and Javaux, M. (2010). Model-assisted integration of physiological and environmental constraints
957   affecting the dynamic and spatial patterns of root water uptake from soils. *Journal of Experimental Botany*, 61(8):2145–2155.

958   Ellis, T., Murray, W., and Kavalieris, L. (2013). Electrical capacitance of bean (Vicia faba) root systems was related to tissue density-a
959   test for the Dalton Model. *Plant and Soil*, 366(1-2):575–584.

960   Everett, M. E. (2013). *Near-surface applied geophysics.* Cambridge University Press.

961   Farzamian, M., Monteiro, F. A., and Khalil, M. A. (2015). Application of EM38 and ERT methods in estimation of saturated hydraulic
962   conductivity in unsaturated soil. *Journal of Applied Geophysics*, 112:175–189.

963   Fukue, M., Minato, T., Horibe, H., and Taya, N. (1999). The micro-structures of clay given by resistivity measurements. *Engineering
964   Geology*, 54:43–53.

965   Furman, A., Arnon-Zur, A., and Assouline, S. (2013). Electrical resistivity tomography of the root zone. In *Soil-Water-Root Processes:
966   Advances in Tomography and Imaging*, pages 223–245. SSSA Special Publications.

967   Garré, S., Coteur, I., Wongleecharoen, C., Kongkaew, T., Diels, J., Vanderborght, J., and Province, R. (2013). Noninvasive Monitoring
968   of Soil Water Dynamics in Mixed Cropping Systems : A Case Study in Ratchaburi Province, Thailand. *Vadose zone journal*, 12:1–12.

969   Garré, S., Günther, T., Diels, J., and Vanderborght, J. (2012). Evaluating Experimental Design of ERT for Soil Moisture Monitoring
970   in Contour Hedgerow Intercropping Systems. *Vadose zone journal*, 11:1–14.

971   Garré, S., Javaux, M., Vanderborght, J., Pagès, L., and Vereecken, H. (2011). Three-Dimensional Electrical Resistivity Tomography to
972   Monitor Root Zone Water Dynamics. *Vadose Zone Journal*, 10(1):412–424.

973   Green, S. R., Kirkham, M. B., and Clothier, B. E. (2006). Root uptake and transpiration: From measurements and models to sustainable
974   irrigation. *Agricultural Water Management*, 86(1-2):165–176.

975   Günther, T., Rucker, C., and Spitzer, K. (2006). Three-dimensional modelling and inversion of dc resistivity data incorporating
976   topography – ii. *Geophysical journal international*, 166:506–517.

977   Guyot, A., Ostergaard, K. T., Lenkopane, M., Fan, J., and Lockington, D. A. (2013). Using electrical resistivity tomography to
978   differentiate sapwood from heartwood : application to conifers. *Tree Physiology*, 33:187–194.

979   Haynes, R. and Beare, M. H. (1997). Influence Stability of Six Crop Species on Aggregate and Some Labile Organic Matter Fractions.
980   *Science*, 29(1):1647–1653.

981   Hill, K., Porco, S., Lobet, G., Zappala, S., Mooney, S., Draye, X., and Bennett, M. J. (2013). Root Systems Biology : Integrative
982   Modeling across Scales , from Gene Regulatory Networks to the Rhizosphere. *Plant Physiology*, 163:1487–1503.

983   Javaux, M., Couvreur, V., Vanderborght, J., and Vereecken, H. (2013). Root Water Uptake : From Three-Dimensional Biophysical
984   Processes to Macroscopic Modeling Approaches. *Vadose Zone Journal*.

985 Jones, G. M., Cassidy, N. J., Thomas, P. A., Plante, S., and Pringle, J. K. (2009). Imaging and monitoring tree-induced subsidence
986   using electrical resistivity imaging. *Near Surface Geophysics*, 7(3):191–206.

987 Kelly, B. F., Acworth, R. I., and Greve, A. K. (2011). Better placement of soil moisture point measurements guided by 2D resistivity
988   tomography for improved irrigation scheduling. *Soil Research*, 49(6):504–512.

989 Kelter, M., Huisman, J. A., Zimmermann, E., Kemna, A., and Vereecken, H. (2015). Quantitative imaging of spectral electrical
990   properties of variably saturated soil columns. *Journal of Applied Geophysics*, 123:333–344.

991 Kemna, A. (2000). *PhD Thesis: Tomographic inversion of complex resistivity – theory and application*. Ruhr-Universitat Bochum.

992 Koestel, J., Dathe, A., Skaggs, T. H., Klakegg, O., Ahmad, M. A., Babko, M., Giménez, D., Farkas, C., Nemes, A., and Jarvis, N.
993   (2018). Estimating the Permeability of Naturally Structured Soil From Percolation Theory and Pore Space Characteristics Imaged
994   by X-Ray. *Water Resources Research*, 54(11):9255–9263.

995 Koestel, J., Kasteel, R., Esser, O., Kemna, A., Javaux, M., and Binley, A. (2007). Imaging brilliant blue stained soil by means of
996   electrical resistivity tomography. *Vadose Zone Journal*, 8:963–975.

997 Koestel, J., Kemna, A., Javaux, M., Binley, A., and Vereecken, H. (2008). Quantitative imaging of solute transport in an unsaturated
998   and undisturbed soil monolith with 3-D ERT and TDR. *Water Resources Research*, 44:1–17.

999 Kowalczyk, S., Zawrzykraj, P., and Mieszkowski, R. (2015). Application of electrical resistivity tomography in assessing complex soil
1000   conditions. *Geological Quarterly*, 59(2):367–372.

1001 Laloy, E., Javaux, M., Vanclooster, M., Roisin, C., and Bielders, C. L. (2011). Electrical Resistivity in a Loamy Soil: Identification of
1002   the Appropriate Pedo-Electrical Model. *Vadose Zone Journal*, 10(3):1023–1033.

1003 Leucci, G. (2010). The use of three geophysical methods for 3d images of total root volume of soil in urban environments. *Exploration
1004   Geophysics*, 41:268–278.

1005 Linde, N., Binley, A., Tryggvason, A., Pedersen, L. B., and Revil, A. (2006). Improved hydrogeophysical characterization using joint
1006   inversion of cross-hole electrical resistance and ground-penetrating radar traveltime data. *Water Resources Research*, 42(12):1–16.

1007 Loke, M. (2018a). *Res2DInv software*. https://www.geotomosoft.com/products.php#3D [Accessed: 18/01/2019].

1008 Loke, M. (2018b). *Res3DInv software*. https://www.geotomosoft.com/products.php#3D [Accessed: 18/01/2019].

1009 Loke, M. and Barker, R. (1995). Least-squares deconvolution of apparent resistivity pseudosections. *Geophysics*, 60(6):1682–1690.

1010 Lu, H.-l., Liu, Z.-d., Zhou, Q., and Xu, R.-k. (2018). Zeta potential of roots determined by the streaming potential method in relation
1011   to their Mn (II) sorption in 17 crops. *Plant and Soil*, 428:241–251.

1012 Lyklema, J., Duhkin, S., and Shilov, D. (1983). The relaxation of the double-layer around colloidal particles and the low-frequency
1013   dielectric-dispersion .1. theoretical considerations. *Journal of Electroanalytical Chemistry*, 1-2:1–21.

1014 Mairhofer, S., Johnson, J., Sturrock, C. J., Bennett, M. J., Mooney, S. J., and Pridmore, T. P. (2016). Visual tracking for the recovery
1015   of multiple interacting plant root systems from X-ray μ CT images. *Machine Vision and Applications*, 27(5):721–734.

1016 Marani, M., Silvestri, S., Belluco, E., Ursino, N., Comerlati, A., Tosatto, O., and Putti, M. (2006). Spatial organization and ecohydro-
1017   logical interactions in oxygen-limited vegetation ecosystems. *Water Resources Research*, 42:1–12.

1018 Mares, R., Barnard, H. R., Mao, D., Revil, A., and Singha, K. (2016). Examining diel patterns of soil and xylem moisture using
1019   electrical resistivity imaging. *JOURNAL OF HYDROLOGY*, 536:327–338.

1020 Marshall, D. J., Madden, T. R., The, A., February, E., and Associates, N. A. (1959). Induced polarization, a study of its causes,.
1021   *Geophysics*, 24(4):790–816.

1022 Martin, T. (2012). Complex resistivity measurements on oak. *European Journal of Wood and Wood Products*, 70(1-3):45–53.

1023 Mary, B., Abdulsamad, F., Saracco, G., Peyras, L., Vennetier, M., Mériaux, P., and Camerlynck, C. (2017). Improvement of coarse root
1024   detection using time and frequency induced polarization: from laboratory to field experiments. *Plant and Soil*, 417(1-2):243–259.

1025 Mary, B., Peruzzo, L., Boaga, J., Schmutz, M., Wu, Y., Hubbard, S. S., and Cassiani, G. (2018). Small-scale characterization of vine
1026   plant root water uptake via 3-D electrical resistivity tomography and mise-à-la-masse method. *Hydrology and Earth System Sciences*,
1027   22:5427–5444.

1028 Mary, B., Saracco, G., Peyras, L., Vennetier, M., Mériaux, P., and Camerlynck, C. (2016). Mapping tree root system in dikes using
1029   induced polarization: Focus on the influence of soil water content. *Journal of Applied Geophysics*, 135:387–396.

1030 Michot, D., Benderitter, Y., Dorigny, A., Nicoullaud, B., King, D., and Tabbagh, A. (2003). Spatial and temporal monitoring of soil
1031   water content with an irrigated corn crop cover using surface electrical resistivity tomography. *Water Resources Research*, 39(5):1–20.

1032 Michot, D., Dorigny, A., and Benderitter, Y. (2001). Mise en évidence par résistivité électrique des écoulements préférentiels et de
1033   l'asséchement par le maïs d'un calcisol de beauce irrigué. *Earth and Planetary Sciences*, 332:29–36.

1034 Mooney, S. J., Pridmore, T. P., Helliwell, J., and Bennett, M. J. (2012). Developing X-ray computed tomography to non-invasively
1035   image 3-D root systems architecture in soil. *Plant and Soil*, 352(1-2):1–22.

1036 Morari, F., Castrignanò, A., and Pagliarin, C. (2009). Application of multivariate geostatistics in delineating management zones within
1037   a gravelly vineyard using geo-electrical sensors. *Computers and Electronics in Agriculture*, 68(1):97–107.

1038 Moreno, Z., Arnon-Zur, A., and Furman, A. (2015). Hydro-geophysical monitoring of orchard root zone dynamics in semi-arid region.
1039   *Irrigation Science*, 33(4):303–318.

1040 Mualem, Y. and Friedman, S. (1991). Theoretical Prediction of Electrical Conductivity in Saturated and Unsaturated soil. *Water
1041   Resources Research*, 27(10):2771–2777.

1042 Musgrave, H. and Binley, A. (2011). Revealing the temporal dynamics of subsurface temperature in a wetland using time-lapse
1043   geophysics. *Journal of Hydrology*, 396(3-4):258–266.

1044 Newill, P., Karadaglí C, D., Podd, F., Grieve, B. D., and York, T. A. (2014). Electrical impedance imaging of water distribution in the
1045   root zone. *Measurement Science and Technology*, 5(25).

1046 Nijland, W., van der Meijde, M., Addink, E., and de Jong, S. (2010). Detection of soil moisture and vegetation water abstraction in a
1047   mediterranean natural area using electrical resistivity tomography. *Catena*, 81(3):209–216.

1048 Olsen, P. A., Binley, A., and Tych, W. (1999). Characterizing solute transport in undisturbed soil cores using electrical and X-ray
1049   tomographic methods. *Hydrological Processes*, 13:211–221.

1050 Ozier-lafontaine, H. and Bajazet, T. (2005). Analysis of Root Growth by Impedance Spectroscopy (EIS) Analysis of root growth by
1051   impedance spectroscopy (EIS). *Plant and Soil*, 255(December):299–313.

1052 Panissod, C., Michot, D., Benderitter, Y., and Tabbagh, A. (2001). On the effectiveness of 2D electrical inversion results: An agricultural
1053   case study. *Geophysical Prospecting*, 49(5):570–576.

1054 Pelton, W., Ward, S., Hallof, P., Sill, W., and PH, N. (1978). Mineral discrimination and removal of inductive coupling with multifre-
1055   quency ip. *Geophysics*, 43:588–609.

1056 Pennell, K. D. (2016). *Reference Module in Earth Systems and Environmental Sciences*. Elsevier.

1057 Peyton, R. L., Haeffner, B. A., Anderson, S. H., and Gantzer, C. J. (1992). Applying X-ray CT to measure macropore diameters in
1058   undisturbed soil cores. *Geoderma*, 53(3-4):329–340.

1059 Postma, J. A., Kuppe, C., Owen, M. R., Mellor, N., Griffiths, M., Bennett, M. J., Lynch, J. P., and Watt, M. (2017). OpenSimRoot:
1060   widening the scope and application of root architectural models. *New Phytologist*, 215:1274–1286.

1061 Pound, M. P., Atkinson, J. A., Townsend, A. J., Wilson, M. H., Griffiths, M., Jackson, A. S., Bulat, A., Tzimiropoulos, G., Wells,
1062   D. M., Murchie, E. H., Pridmore, T. P., and French, A. P. (2017). Deep machine learning provides state-of-the-art performance in
1063   image-based plant phenotyping. *GigaScience*, 6(10):1–10.

1064 Rao, S., Meunier, F., Ehosioke, S., Lesparre, N., Kemna, A., Nguyen, F., Garré, S., and Javaux, M. (2018). A mechanistic model for
1065   electrical conduction in soil-root continuum: a virtual rhizotron study. *Biogeosciences Discussions*.

1066 Revil, A. (1999). Ionic diffusivity, electrical conductivity, membrane and thermoelectric potentials in colloids and granular porous media:
1067   A unified model. *Journal of Colloid and Interface Science*, 212:503–522.

1068 Revil, A., Cathles, L. M., Losh, S., and Nunn, J. a. (1998). Electrical conductivity in shaly sands with geophysical applications. *Journal
1069   of Geophysical Research*, 103:23925–23936.

1070 Revil, A. and Glover, P. (1997). Theory of ionic-surface electrical conduction in porous media. *Physical Review B - Condensed Matter
1071   and Materials Physics*, 55(3):1757–1773.

1072 Rhoades, J., Manteghi, N., Shouse, P., and Alves, W. (1989). Soil electrical conductivity and soil salinity: new formulations and
1073   calibrations. *Soil Science Society of America*, 53:433–439.

1074 Robinson, J. L., Slater, L. D., and Schäfer, K. V. (2012). Evidence for spatial variability in hydraulic redistribution within an oak-pine
1075   forest from resistivity imaging. *Journal of Hydrology*, 430-431:69–79.

1076 Romero-Ruiz, A., Linde, N., Keller, T., and Or, D. (2018). A Review of Geophysical Methods for Soil Structure Characterization.
1077   *Reviews of Geophysics*, 56(4):672–697.

1078 Rossi, R., Amato, M., Bitella, G., Bochicchio, R., Ferreira Gomes, J. J., Lovelli, S., Martorella, E., and Favale, P. (2011). Electrical
1079   resistivity tomography as a non-destructive method for mapping root biomass in an orchard. *European Journal of Soil Science*,
1080   62(2):206–215.

1081 Sabo, D., McMurray, G., and Rains, G. (2016a). Presymptomatic Disease Detection and Nanoparticle-Enhanced Electrical Capacitance
1082   Tomography. *IFAC-PapersOnLine*, 49(16):116–120.

1083 Sabo, D., McMurray, G., and Rains, G. (2016b). Root monitoring system using electrical capacitance tomography (ect) for pre-
1084   symptomatic disease detection. *ASABE Annual International Meeting*.

1085 Samouëlian, A., Cousin, I., Tabbagh, A., Bruand, A., and Richard, G. (2005). Electrical resistivity survey in soil science : a review.
1086   *Soil and Tillage Research*, 83:173–193.

1087 Schnepf, A., Leitner, D., Landl, M., Lobet, G., Hieu, T., Morandage, S., Sheng, C., Zörner, M., and Vanderborght, J. (2017). CRootBox
1088   : A structural-functional modelling framework for root systems. *Annals of Botany*, 121(5):1033–1053.

1089 Schwan, H. (1957). Electrical properties of tissue and cell suspensions. *Advances in Biological and Medical Physics*, 5:147–209.

1090 Schwartz, N. and Furman, A. (2015). On the spectral induced polarization signature of soil organic matter. *Geophysical journal
1091   international*, 200:589–595.

1092   Segal, E., Kushnir, T., Mualem, Y., and Shani, U. (2008). Water Uptake and Hydraulics of the Root Hair Rhizosphere. *Vadose Zone*
1093   *Journal*, 7(3):1027–1034.

1094   Srayeddin, I. and Doussan, C. (2009). Estimation of the spatial variability of root water uptake of maize and sorghum at the field scale
1095   by electrical resistivity tomography. *Plant and Soil*, 319(1-2):185–207.

1096   Topp, G., Davis, J., and Annan, A. (1980). Electromagnetic determination of soil water content: Measurements in coaxial transmission
1097   lines. *Water Resources Research*, 14:574–582.

1098   Tosatto, O., Belluco, E., Silvestri, S., Ursino, N., Comerlati, A., Putti, M., and Marani, M. (2009). Reply to comment by L . R .
1099   Gardner on " Spatial organization and ecohydrological interactions in oxygen-limited vegetation ecosystems ". *Water Resources*
1100   *Journal*, 45:2–5.

1101   Ursino, N., Cassiani, G., Deiana, R., Vignoli, G., and Boaga, J. (2014). Measuring and modeling water-related soil-vegetation feedbacks
1102   in a fallow plot. *Hydrology and Earth System Sciences*, 18(3):1105–1118.

1103   van Genuchten, M. T. (1980). A closed form equation for predicting the hydraulic conductivity of unsaturated soils. *Soil Science Society*
1104   *of America*, 44:892–898.

1105   Vanderborght, J., Huisman, J., Kruk, J., and Vereecken, H. (2013). Geophysical methods for field-scale imaging of root zone properties
1106   and processes. In *Soil-Water-Root Processes: Advances in Tomography and Imaging*, pages 247–282. SSSA Special Publications.

1107   Vrugt, J., Hopmans, J., and Simunel, J. (2001). Calibration of a Two-Dimensional Root Water Uptake Model. *Soil Science Society of*
1108   *America*, 65(4):1027–1037.

1109   Wang, B., Ji, H., and Hu, Y. (2012). A novel electrical resistance tomography system based on (cd)-d-4 technique. *29th Annual IEEE*
1110   *International Instrumentation and Measurement Technology Conference*.

1111   Waxman, M. and Smits, L. (1968). Electrical conductivities in oil-bearing shaly sands. *Society of Petroleum Engineers Journal*,
1112   243:107–122.

1113   Weigand, M. and Kemna, A. (2016). Debye decomposition of time-lapse spectral induced polarisation data. *Computers and Geosciences*,
1114   86:34–45.

1115   Weigand, M. and Kemna, A. (2017). Multi-frequency electrical impedance tomography as a non-invasive tool to characterize and
1116   monitor crop root systems. *Biogeosciences*, 14(4):921–939.

1117   Weigand, M. and Kemna, A. (2018). Imaging and functional characterization of crop root systems using spectroscopic electrical
1118   impedance measurements. *Plant and Soil*, 435:201–224.

1119   Werban, U., Al Hagrey, S. A., and Rabbel, W. (2008). Monitoring of root-zone water content in the laboratory by 2D geoelectrical
1120   tomography. *Journal of Plant Nutrition and Soil Science*, 171(6):927–935.

1121   Whalley, W. R., Binley, A., Watts, C. W., Shanahan, P., Dodd, I. C., Ober, E. S., Ashton, R. W., Webster, C. P., White, R. P., and
1122   Hawkesford, M. J. (2017). Methods to estimate changes in soil water for phenotyping root activity in the field. *Plant and Soil*,
1123   415(1-2):407–422.

1124   Wu, S. Y., Zhou, Q. Y., Wang, G., and Liu, T. M. (2013). Response characteristics and tomographic monitoring of the electric
1125   capacitance after irrigation in the soil-plant (ginkgo tree) continuum in a laboratory. *Environmental Earth Sciences*, 68(3):655–666.

1126   Zanetti, C., Weller, A., Vennetier, M., and Mériaux, P. (2011). Detection of buried tree root samples by using geoelectrical measurements:
1127   A laboratory experiment. *Plant and Soil*, 339(1):273–283.

1128 Zelazny, L., He, L., and Vanwormhoudt, A. M. (1996). Charge alanyses of soils and anion exchange. *Methods of soil analysis, Part*
1129   *3-Chemical methods*, pages 1231–1255.

1130 Zenone, T., Gianfranco, M., Maurizio, T., Federico, F., Marco, M., Matteo, S., Alessio, A., Chiara, F., Tommaso, C., and Guenther,
1131   S. (2008). Preliminary use of ground-penetrating radar and electrical resistivity tomography to study tree roots in pine forests and
1132   poplar plantations. *Functional plant biology*, 35:1047–1058.

1133 Zimmermann, E., Kemna, A., Berwix, J., Glaas, W., and Vereecken, H. (2008). EIT measurement system with high phase accuracy for
1134   the imaging of spectral induced polarization properties of soils and sediments. *Measurement Science and Technology*, 19(9):094010.

1135   **Figure captions**:

1136   Figure 1. Diagram of key theoretical characteristics associated to geoelectrical methods described. The dotted line

1137   connects the scheme branch with the corresponding geoelectrical method.

1138   Figure 2. Laboratory set-up of a geoelectrical soil column monitoring experiment A) Soil column lateral view B)

1139   Horizontal Cross-section view. Adapted from Garré et al. (2011), (Koestel et al., 2007).

1140   Figure 3. Three dimensional solute concentration distribution in 6 stages of infiltration. Corresponding time-steps

1141   are listed in the top-left corner. Extracted from Koestel et al. (2008).

1142   Figure 4. Field acquisition pseudosection line used for ERT surveys. Electrodes are grouped in a Dipole-Dipole

1143   sequence.

1144   Figure 5. 2D ERT field resistivity distribution variation with time under crops of Maize left and Sorghum right.

1145   Extracted from Srayeddin and Doussan (2009).

1146   Figure 6. Resistivity increment percent differences overlapped on 3D rendering of laser-scan point cloud of Pinus

1147   Pinea root system. a) 3D view b) 25 cm below surface c) vertical section. Extracted from Zenone et al. (2008).

1148   Figure 7. Bar chart indicating number of published articles which use Geoelectrical monitoring methods for the

1149   study of root zone processes.

1150   Figure 8. Schematic representation extracted from Postma et al. (2017) representing the model used that couples

1151   evapotranspiration, xylem transport and soil water dynamics. a) Soil pedon with the hydraulic head indicated in

1152   pseudo-color (left) and three barley root systems (right) taking up water from that column. b) Penman– Monteith

1153   equation was used for the simulation of transpiration and evaporation. c) Section of the simulated root network

1154   showing its edges and vertices d) Network model used for the simulation of water flow through the roots (Alm et al.,

1155   1992) e) Water transport in three dimensions in the soil was simulated by solving the Richards equation, which

1156   combines Darcy's law with mass conservation, using the finite element method.

1157   Figure 9. Stages of an indersciplinary strategy to perfect root zone geoelectrical monitoring and corresponding

1158   conceptual models. In blue: Main steps of the strategy flowchart; In green: Existent auxiliary methods or models

1159   that can be used; In orange: Mathematical algorithms needed; Black arrow: Indicates the step succession; Dashed

1160   double arrow: Underlines the need of consistency between the two steps; Orange double arrow: Implies a comparison

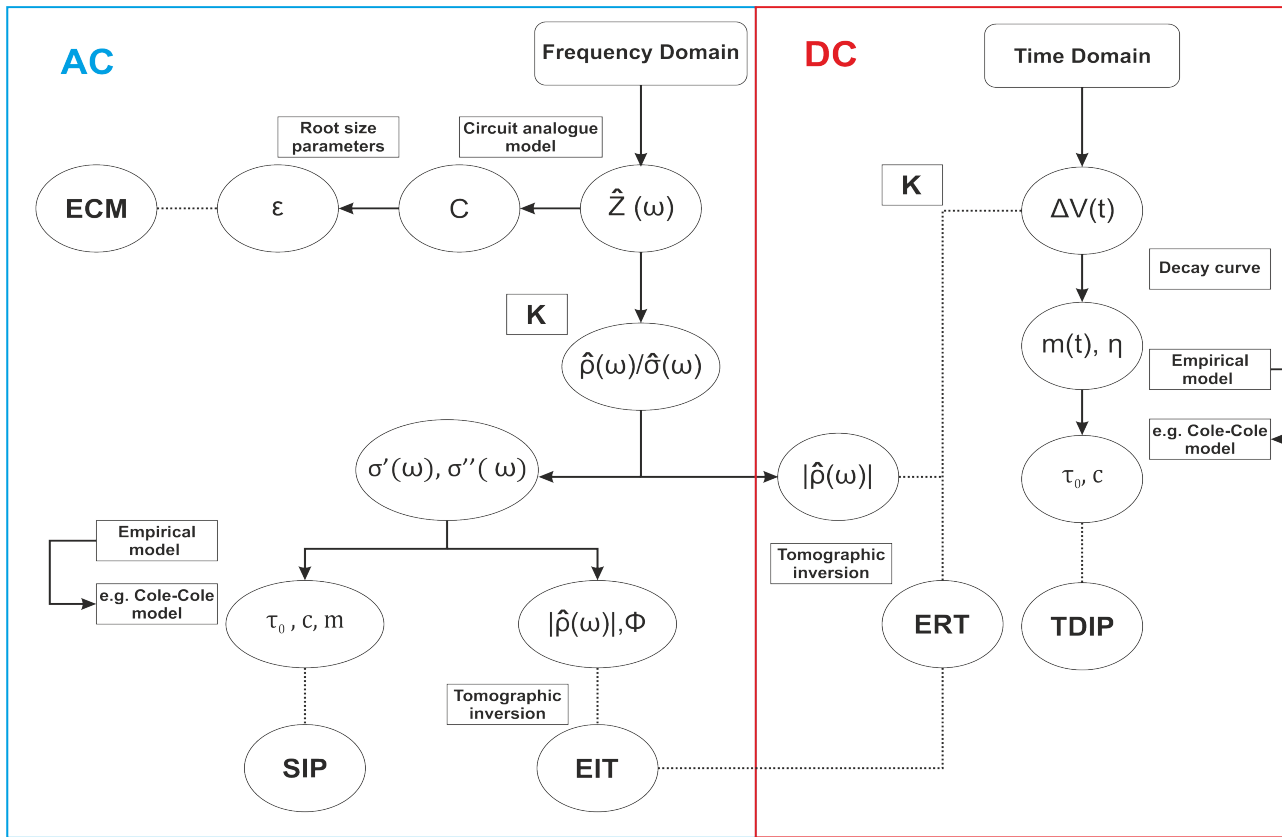1161   between the results.

1162   Note. Colour should be used for all the figures in print.
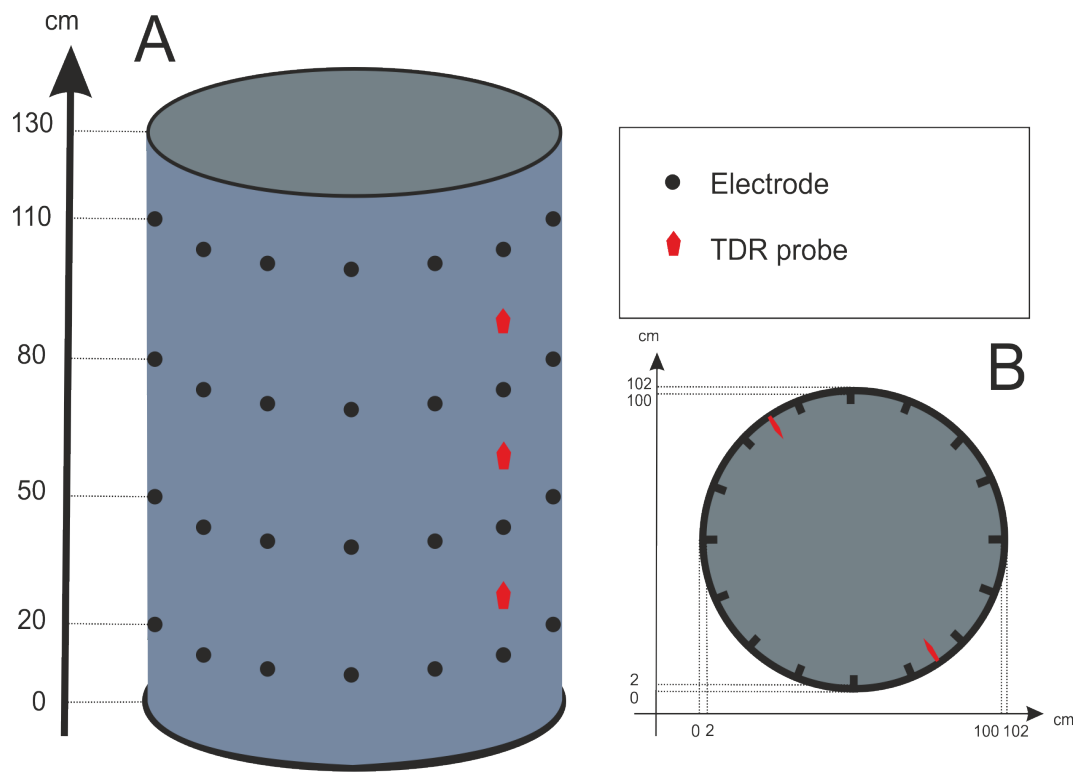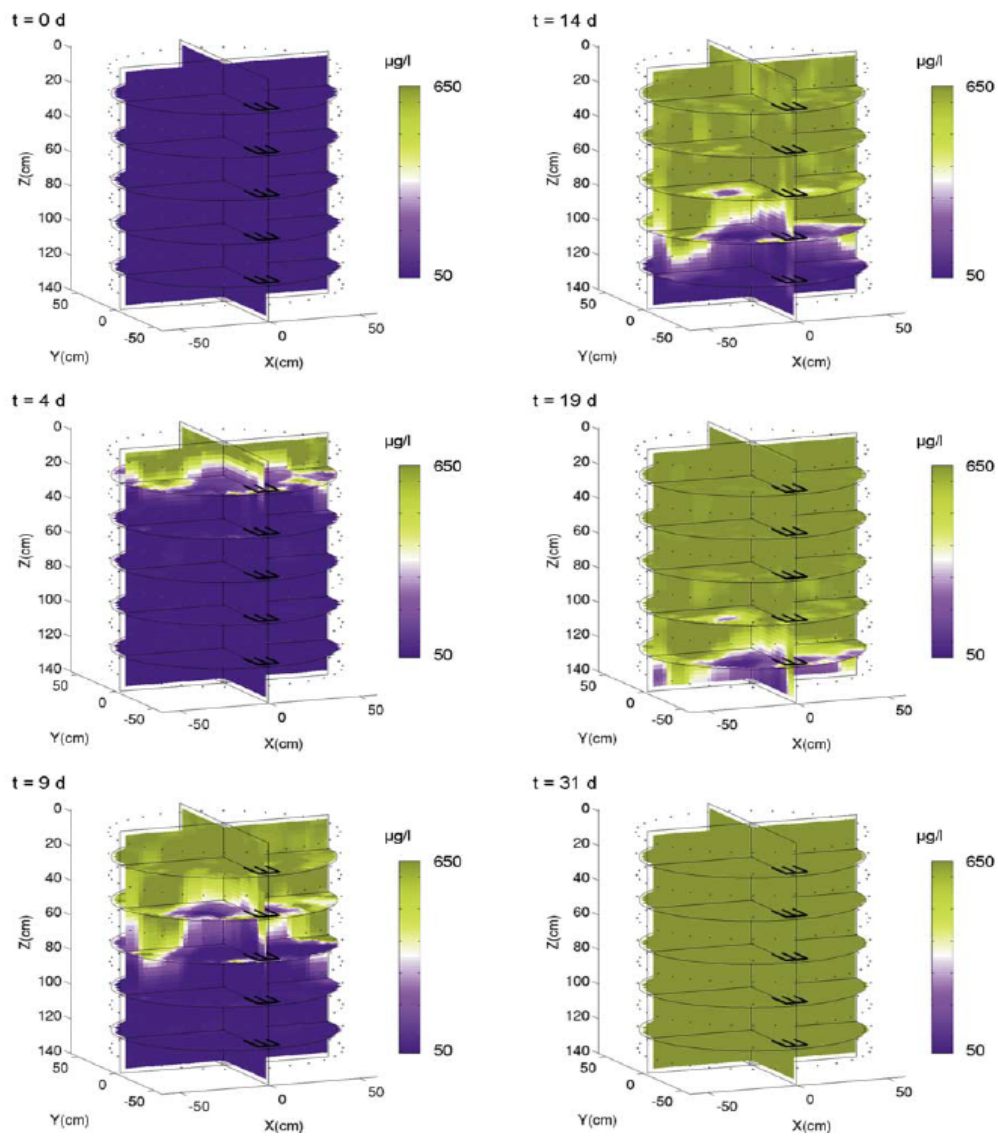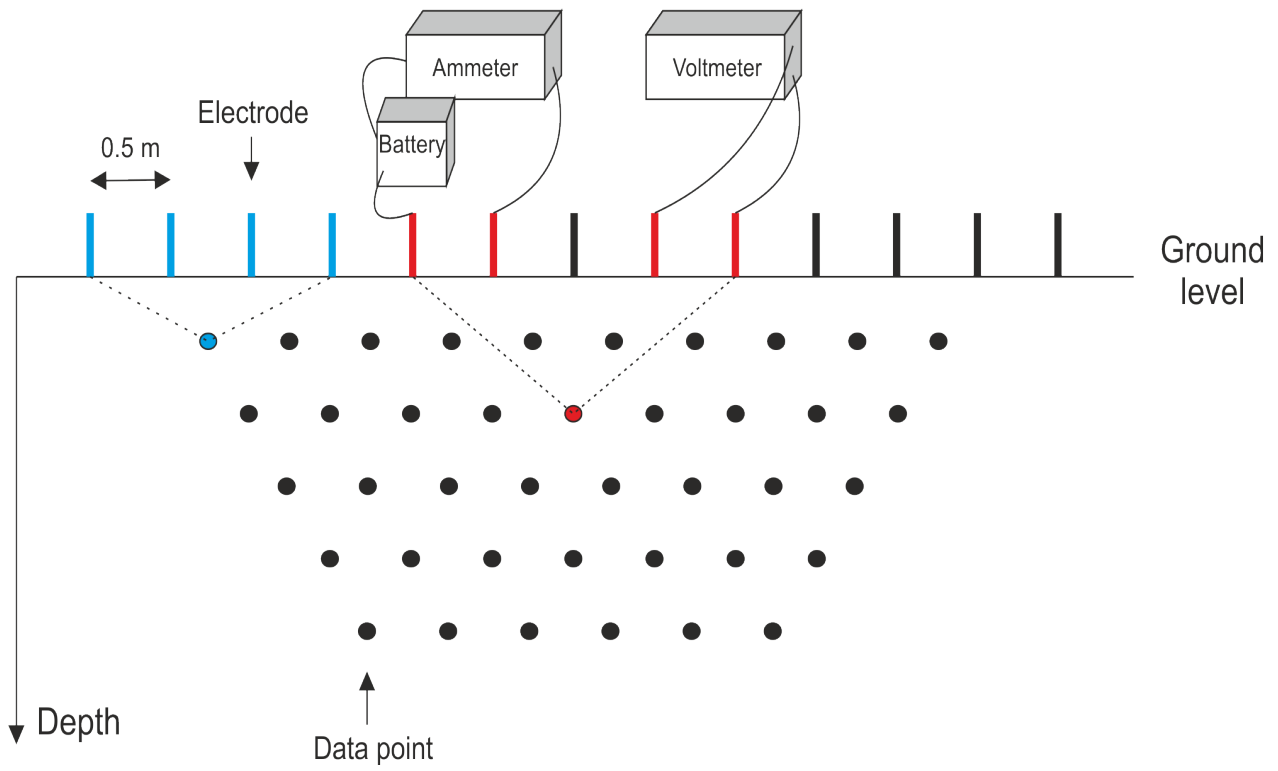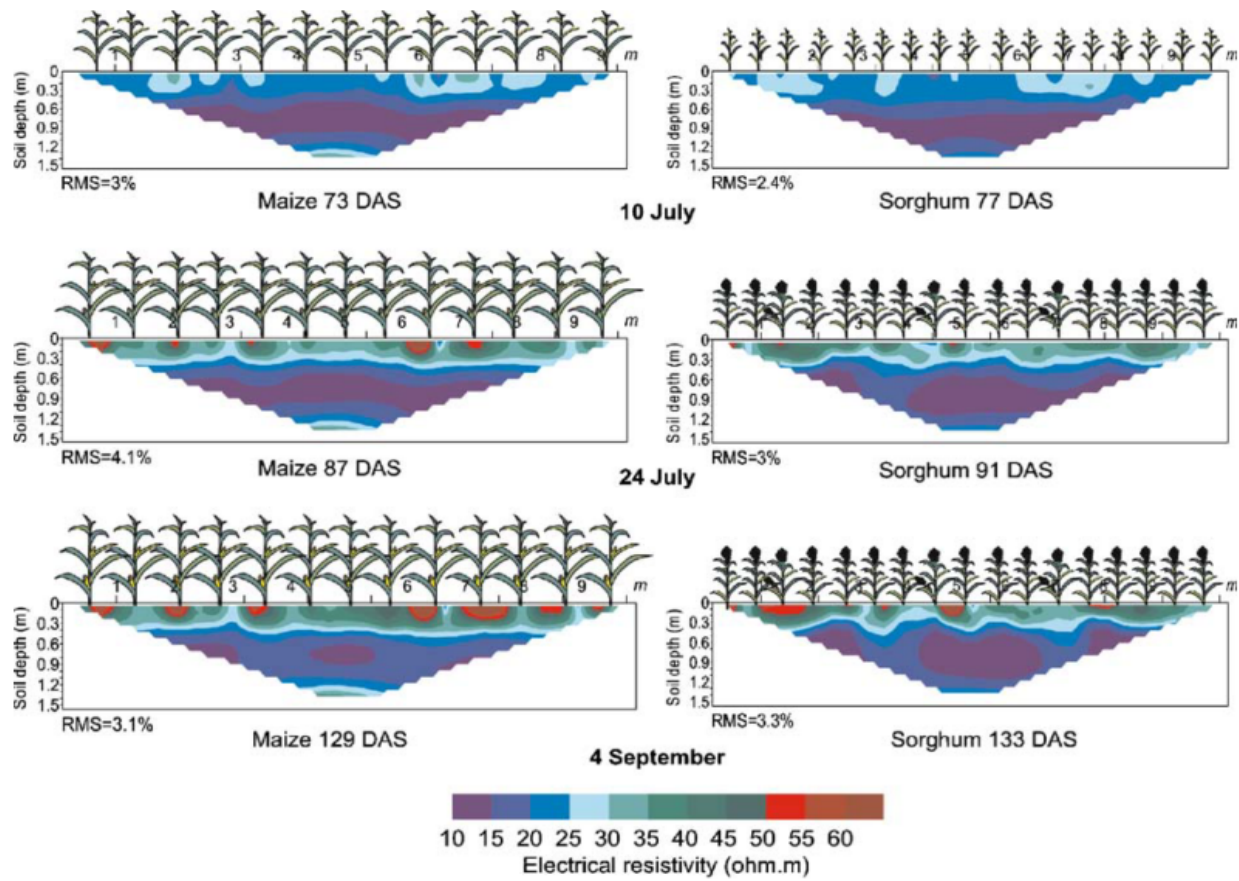
Figure 1

Figure 2

Figure 3

Figure 4

10 July

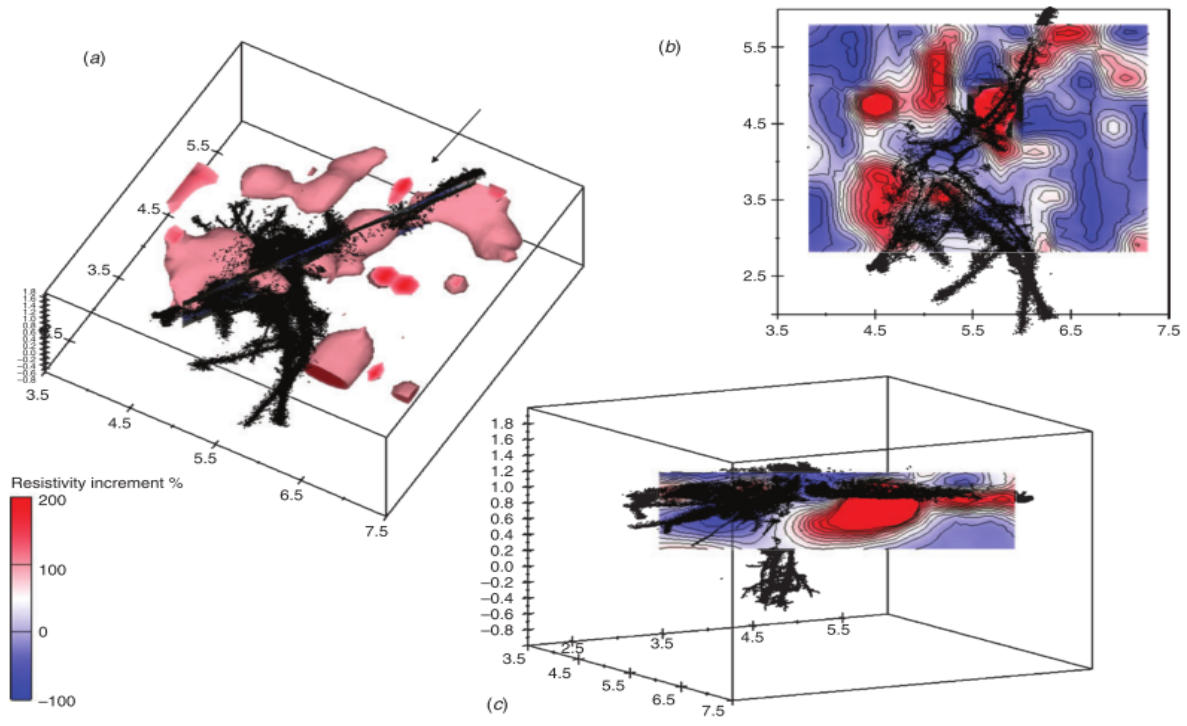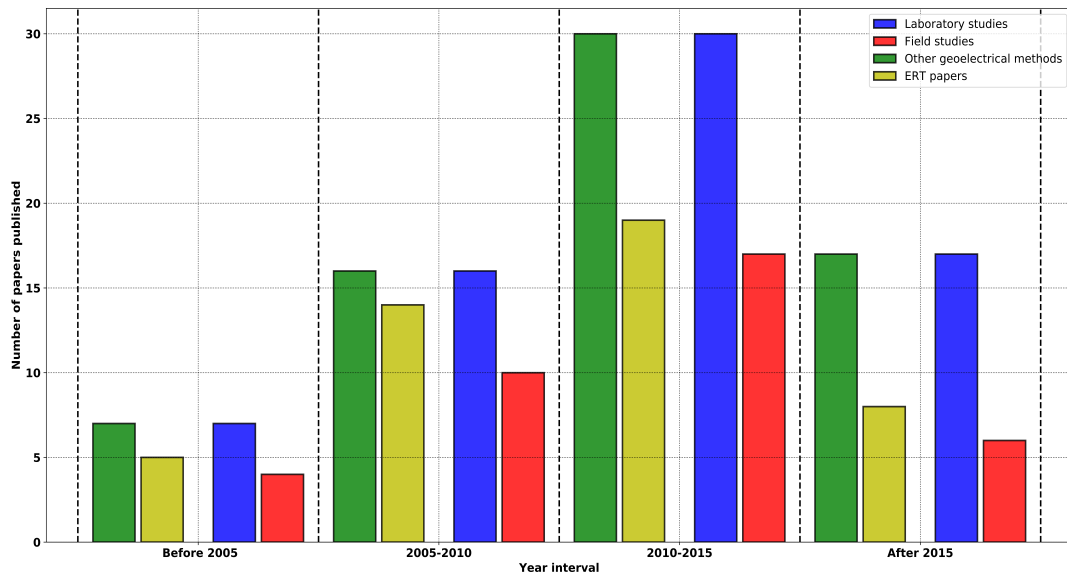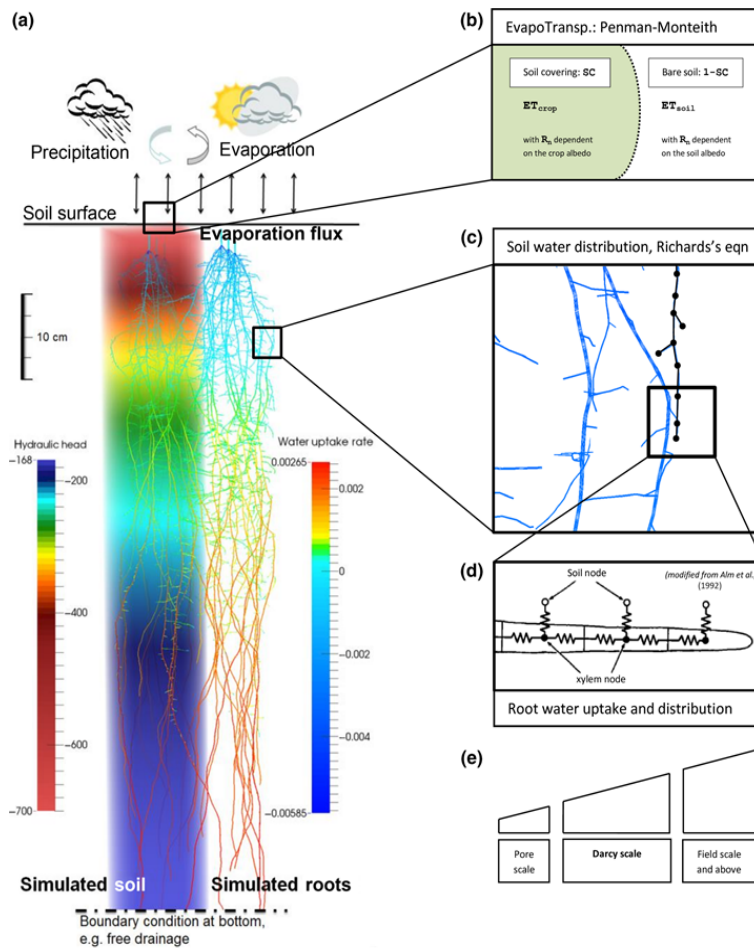24 July

4 September

Figure 5

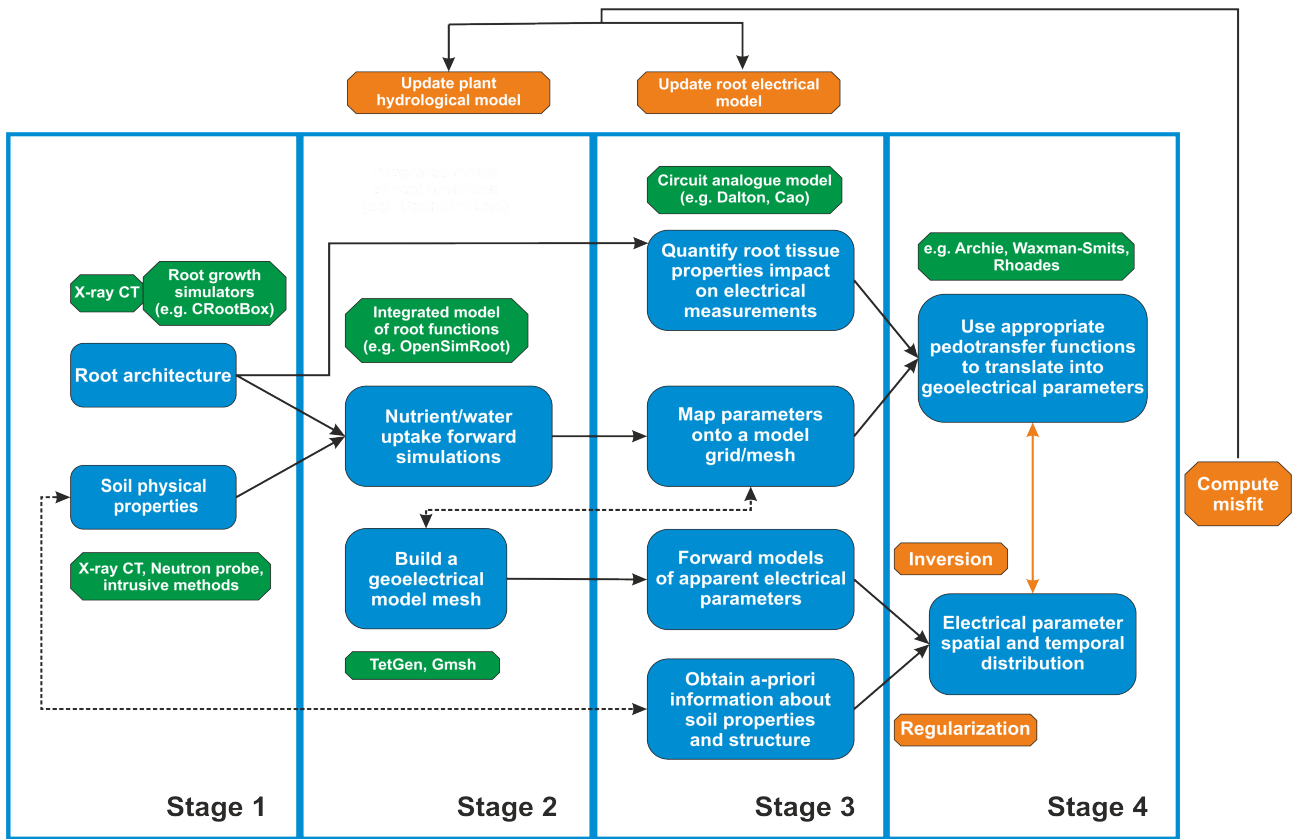Figure 6

Figure 7

Figure 8

Figure 9

1163 Appendix A

Authors, year	Study environement	Geoelectric method	Dimensionality	Acquisition equipment/ Inversion algorithm	Complementary method
Amato, 2008	Field	ERT	2D	Geostudi Astier / Occam's inversion	Destructive samples
Amato, 2009	Laboratory	ERT	3D	Iris Syscal Pro ten-channel receiver / Occam's inversion	Destructive samples
Aulen and Shipley,2012	Laboratory	EC	1D	BK Precision 879	Destructive samples
Basso, 2010	Field	ERT	2D	Iris instruments / Tomolab inversion	soil resistance to penetration data
Beff, 2013	Field	ERT	3D	SYSCAL Pro instrument / BERT Günther et al. (2006)	TDR
Binley,1996	Laboratory	ERT	3D	UMIST Mk1b/Inversion algorithm explained in article	-
Boaga, 2014	Field	ERT	2D	IRIS Syscal Pro / R2T code Binley (2018a)	tensiometer
Boaga, 2013	Field	ERT	3D	IRIS Syscal Pro 72 / R3T Binley (2018b)	TDR
Brillante, 2014	Field	ERT	3D	Syscal Junior Switch 48 / RES2DINV	TDR
Brillante, 2016 a	Field	ERT	2D	Syscal Junior Switch 48 / RES2DINV Loke (2018a)	TDR, Pre-dawn leaf water potential
Brillante, 2016 b	Field	ERT	3D	Syscal Junior Switch 48 / RES2DINV	TDR, Pre-dawn leaf water potential
Cao, 2010	Laboratory	ER	1D	Fluke 8022A Multimeter / -	-
Cao, 2011	Laboratory	EIS	1D	SI1260/-	-
Cassiani, 2016	Field	ERT	3D	IRIS Syscal Pro / R3T	TDR
Cassiani, 2015	Field	ERT	3D	- / R3T	Sap flow and evapotranspiration

Cassiani, 2012	Field	ERT	2D	- / Occam inversion R,R2,R3T	EMI, TDR
Cassiani, 2009	Laboratory	SIP	1D	ZELSIP04/-	X-ray micro CT
Celano, 2011	Field	ERT	2D	Iris Syscal Pro / TomoLab/	Soil sample analysis
Celano, 2010	Field	ERT	2D	Iris Syscal Pro / TomoLab/	Soil sample analysis
Cermak,2006	Field	ER	1D	Megger/-	
Consoli, 2017	Field	ERT	3D	Iris Syscal Pro Switch 72 / Occam R3T	Sap flow
Cseresnyés, 2012	Laboratory	EC/EI	1D	HP 4284A LCR bridge/-	-
Cseresnyés, 2013	Laboratory	EC/EI	1D	HP 4284A LCR bridge/-	-
Cseresnyés, 2014	Laboratory	EC	1D	GW-8101G precision LCR instrument/-	-
Cseresnyés, 2016	Laboratory	EC	1D	GW-8101G precision LCR instrument/-	-
Cseresnyés, 2018	Laboratory/ Field	EC	1D	Agilent U1733C handheld LCR meter/-	TDR
Dietrich, 2012	Laboratory	EC	1D	Passive Component LCR Meter Extech Instruments/-	-
Ellis, 2012	Laboratory	EC	3D	MOTECH YMT-4080D/-	Destructive samples
Fan, 2015	Field	ERT	2D	SYSCAL Pro Switch / RES2DINV	TDR
Garré, 2013	Field	ERT	2D	Syscal Pro resistivity meter /	TDR
Garré, 2012	Field	ERT	2D	Iris Syscal Pro/ Gimli code	TDR
Garré, 2011	Laboratory	ERT	3D	RESECS prototype / Occam inversion	TDR, minirhizotrons
Guyot, 2013	Laboratory	ERT	2D	Picus TreeTronic / Picus Software	Macroscopic analysis of wood moisture an wood density
Jones, 2009	Field	ERT	2D	Campus Tigre 32/64 / RES2DINV	Levelling stations, neutron probe monitoring
Kelly, 2011	Field	ERT	2D	ABEM SAS 4000 Terrameter system / RES2DINV	C-probe
Kelter, 2015	laboratory	EIT	3D	Equipment and inversion developed in Zimmermann et al. (2008)	-

Koestel, 2007	Laboratory	ERT	3D	-/inversion by Binley (1995)	TDR
Koestel, 2008	Laboratory	ERT	3D	GeoServe RESECS/Occam inversion	TDR
Kowalczyk, 2015	Field	ERT	2D	ABEM system / RES2DINV	RCPT sounding
Kuhl, 2018	Laboratory	ER	1D	-/Joined hydrogeophysical inversion algorithm	Hydrological modelling, Plant parameter modelling
Leucci, 2010	Field	ERT	2D/3D	Iris Syscal R1 / RES3DINV Loke (2018b)	GPR, seismic refraction tomography
Lu, 2018	Laboratory	Zeta potential	1D	-/-	CEC;Surface charge measurements
Mares, 2016	Field	ERT	3D	IRIS Syscal Pro Switch 96/R2	Sap flow measurements
Martin, 2012	Laboratory	SIP	1D	SIP 256C / -	-
Mary, 2016	Laboratory	IP	2D	Lippmann Geophysical instrument and Terrameter / RES2DINV	Destructive samples
Mary, 2017	Laboratory	IP/SIP/TDIP	2D	COMSOL Multiphysics , LIPPMANN instrument / Matlab code	-
Mary, 2018	Field	ERT	3D	IRIS Syscal Pro Switch 72/R3T	MALM
Michot, 2003	Field	ERT	2D	Iris Instruments / RES2DINV	TDR
Michot, 2001	Field	ERT	2D	Iris Instruments / RES2DINV	TDR
Morari, 2009	Field	ERT	2D	Iris-Syscal Pro resistivity / ERTLab software	EMI, sampling
Moreno, 2015	Field	ERT	2D	Syscal Pro Switch 96 / R2 software	TDT(time domain transmittance)
Musgrave, 2011	Field	ERT	2D	Geopulse Resistance meter/Occam type inversion	GPR, temperature probes
Newill, 2014	Laboratory	EIT	2D	Hewlett Packard 4192A /-	Compaction measurements
Njland, 2010	Field	ERT	2D	EarthImager2D / AGI algorithms	Soil sampling

Ozier-Lafontaine and Bajazet, 2005	Laboratory	SIP	1D	HP 4992 Impedence Analyzer/-	-
Panissod, 2001	Field	ERT	2D	- / RES2DINV	-
Rao, 2018	Laboratory	ERT	2D	EIDORS electrical modelling	WC modelling; SMARTROOT - root image analyzing tool
Robinson, 2012	Field	ERT	3D	A10 channel instrument / R3	Temperature probes
Rossi, 2011	Field	ERT	2D	Iris Syscal Pro 10 / Tomolab software	Destructive sampling
Sabo, 2016a	Laboratory	EC	1D	BK Precision 879B LCR	-
Sabo, 2016b	Laboratory	EC	1D	BK Precision 879B LCR	-
Srayeddin and Doussan, 2009	Field	ERT	2D	Terrameter SAS 4000 / RES2DINV	Neutron probe and tensiometer measurements
Thierry, 2001	Laboratory	IP	2D	LIPPMANN instrument	-
Ursino, 2014	Field	ERT	2D	- / ProfileR/R2/R	TDR
Weigand, 2017	Laboratory	EIT	2D	EIT-40 / Kemna inversion code Kemna (2000)	-
Weigand and Kemna, 2018	Laboratory	sEIT and EIS	2D	EIT40/CRTomo	-
Werban, 2008	Laboratory	ERT	2D	- / 2D FD-algorithm Loke and Barker (1995)	TDR
Whalley, 2016	Field	ERT	2D	Iris Syscal Pro electrical resistivity meter /inversion strategy in appendix	EMI, neutron probe, penetrometer
Wu, 2013	Laboratory	EC	2D	LCR meter/-	-
Zanetti, 2011	Laboratory	SIP	2D	SIP Fuchs equipment / -	-
Zenone, 2008	Field	ERT	3D	- / ERTLab software	GPR
Zimmerman, 2008	Laboratory	EIT	2D	LABview and MATLAB / Kemna algorithm	-

1164 **Appendix B**

Authors, year	Area of focus	Pedotransfer model	Plant-soil interaction model
Amato, 2008	Plan organic material detection	No	Root mass density logistical growth model
Amato, 2009	Plant organic material detection	No	Regression model
Aulen and Shipley,2012	Plant organic material detection	No	Regression model
Basso, 2010	Root zone water dynamics	Statistical regression model	No
Beff, 2013	Root zone water dynamics	WS	Mualen van Genuchten model (van Genuchten, 1980)
Binley, 1996	Root zone water dynamic	No	Dispersion model
Boaga, 2014	Root zone water dynamics	No	Compared with Marani et al. (2006)
Boaga, 2013	Root zone water dynamics	Archie	No
Brillante, 2014	Root zone water dynamics	Field based function	Pedotransfer model between ER and Soil volume wetness (SVW)
Brillante, 2016 a	Root zone water dynamics	Pedotransfer model obtained by machine learning methods	Soil volume wetness (SVW) available soil water(ASW) and fraction of transpirable soil water (FTSW)
Brillante, 2016 b	Root zone water dynamics	Pedotransfer model obtained by machine learning methods	ASW, FTSW, total transpirable soil water TTSW
Cao,2010	Plant organic material detection	No	Plant system electrical circuit analogue
Cao,2011	Plant organic material detection	No	Plant system electrical circuit analogue
Cassiani, 2016	Root zone water dynamics	Archie	Richards equation modelling
Cassiani, 2015	Root zone water dynamics	Laboratory calibration based on Archie	Van Genuchten model parametrization 1D Richards equation simulations
Cassiani, 2012	Root zone water dynamics	WS	Model of two mass balance equations: 1 for soil moisture, 1 for biomass
Cassiani, 2009	Soil contaminant dynamics	Fit to a Cole-Cole model	No
Celano, 2011	Root zone water dynamics	Laboratory calibration	No

Celano, 2010	Root zone water dynamics	No	Model relating hydraulics saturation, depth and electrical resistivity
Cermak, 2006	Root organic material detection	No	No
Consoli, 2017	Root zone water dynamics	On site calibration	No
Cseresnyés, 2012	Root organic material detection	No	No
Cseresnyés, 2013	Root organic material detection	No	No
Cseresnyés, 2014	Root organic material detection	No	No
Cseresnyés, 2016	Root organic material detection	No	No
Cseresnyés, 2018	Root organic material detection/ WC monitoring	No	Regression model
Dietrch, 2012	Plant organic material detection	No	Root electrical circuit analogue model
Ellis, 2012	Plant organic material detection	No	Compared data with Dalton model — Produced an empirical model
Fan, 2015	Root zone water dynamics	Archie	Derive capacitance model
Garré, 2013	Root zone water dynamics	WS	Hydrological model
Garré, 2012	Root zone water dynamics	WS	No
Garré, 2011	Root zone water dynamics	Simplified WS	No
Guyot, 2017	Sapwood-heartwood electrical differentiation	No	No
Jones, 2009	Tree induced subsidence	No	Tree subsidence model
Kelly, 2011	Root zone water dynamics	Revil model	No
Kelter, 2015	Laboratory soil water dynamics	No	No
Koestel, 2007	Synthetic water dynamics	Laboratory Calibration based on Revil	No
Koestel, 2008	Solute transport	Laboratory Calibration based on Revil	No

Kowalczyk, 2015	Soil peat horizon detection	No	No
Kuhl, 2018	Soil hydraulic parameters, Root parameters and Pedotransfer parameters estimation	Archie	SALUS and HYDRUS and FWD2-5D and SCE-UA
Leucci, 2010	Plant organic material detection	No	No
Lu, 2018	Differentiate between legume and non-legume roots	No	No
Mares, 2016	Root zone water dynamics	No	No
Martin, 2012	Oak impedance signature	No	Simple model based on a system with two parallel pathway for electrical charges (Marshall et al., 1959)
Mary, 2016	Plant organic material detection	No	No
Mary, 2017	Plant organic material detection	No	Cole-Cole model (Cole and Cole, 1941)
Mary, 2018	Plant organic material detection	No	Voltage forward modelling
Michot, 2003	Root zone water dynamics	Field calibration	No
Michot, 2001	Root zone water dynamics	Regression model calibration	No
Morari, 2009	Management zone delimitation	No	Linear model of coregionalisation
Moreno, 2015	Root zone water dynamics	Archie and WS	Model solute transport; separate soil WC from soil water salinity
Musgrave, 2011	Root zone water dynamics	No	No
Newill, 2014	Root zone water dynamics	No	Extend the Wang model (Wang et al., 2012)
Njland, 2010	Root zone water dynamics	Archie based calibration	No

Ozier-Lafontaine and Bajazet, 2005	Plant organic material detection	No	Root circuit analogue model
Panissod, 2001	Root zone water dynamics	No	No
Rao, 2018	Root zone water dynamics	Archie	Root zone water flow modelling
Robinson, 2012	Root zone water dynamics	No	No
Rossi, 2011	Plant organic material detection	No	Regression model — Compare with (Amato et al., 2008) model
Sabo, 2016a	Root health	No	No
Sabo, 2016b	Root health	No	No
Srayeddin and Doussan, 2009	Root zone water dynamics	In situ calibration	No
Thierry, 2001	Wood polarization effect	No	No
Ursino, 2014	Root zone water dynamics	No	Water balance model
Weigand, 2017	Plant organic material detection	No	No
Weigand and Kemna, 2018	Plant organic material detection	No	No
Werban, 2008	Root zone water dynamics	No	No
Whalley, 2016	Root phenotyping	Calibration with neutron probe measurements	No
Wu, 2013	Root zone water dynamics	No	No
Zanetti, 2011	Plant organic material detection	No	No
Zenone, 2008	Plant organic material detection	No	No
Zimmerman, 2008	Soil polarization properties	No	No

1165 **Funding declaration**:

1171